Timing and 4D pixel sensors

unraveling the tangle in particle tracking at extreme rates

19th SEMINAR ON SOFTWARE FOR NUCLEAR, SUBNUCLEAR AND APPLIED PHYSICS

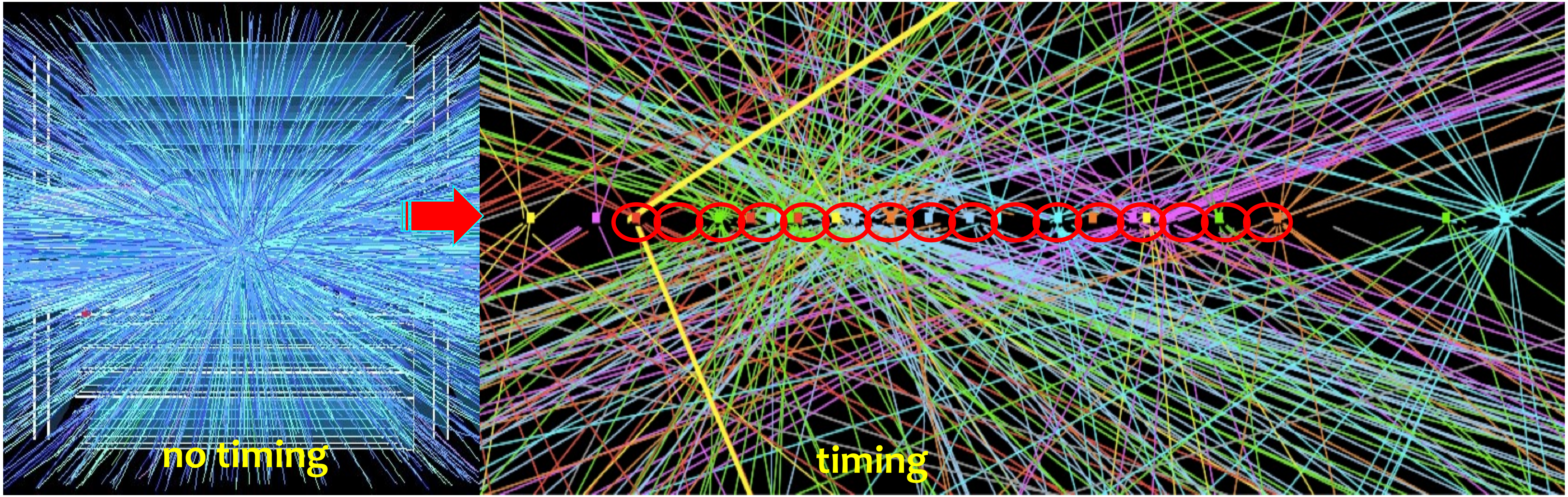

Adriano Lai

INFN CAGLIARI
Istituto Nazionale di Fisica Nucleare
Sezione di Cagliari

4D trackers: what do we mean for?

(beyond pile-up mitigation: when timing layers are not enough)

Plots from:
Considerations for the VELO detector at the LHCb Upgrade II – CERN-LHCb-2022-001

B_{0s} meson decaying into a μ^+ and μ^- pair

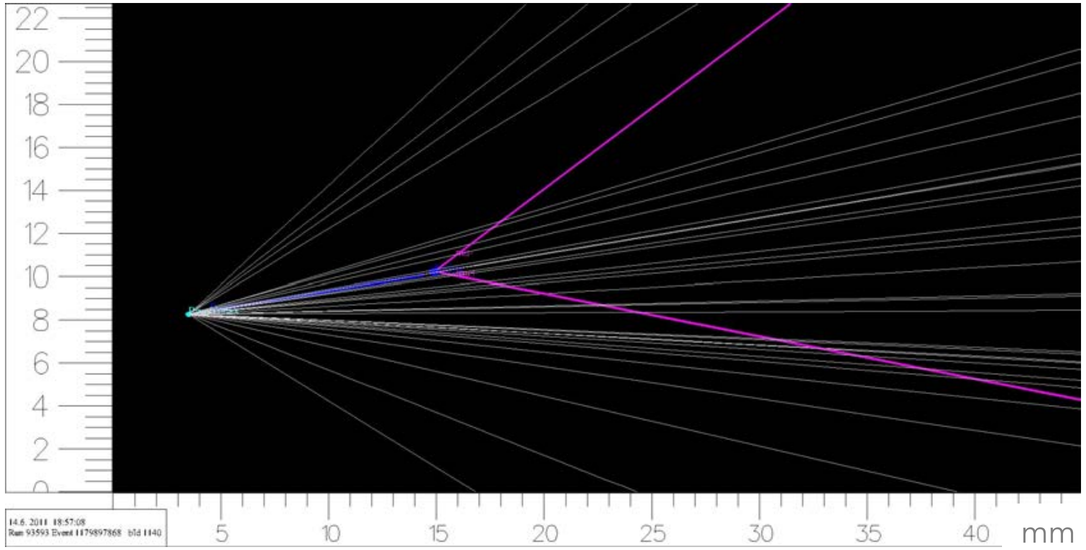

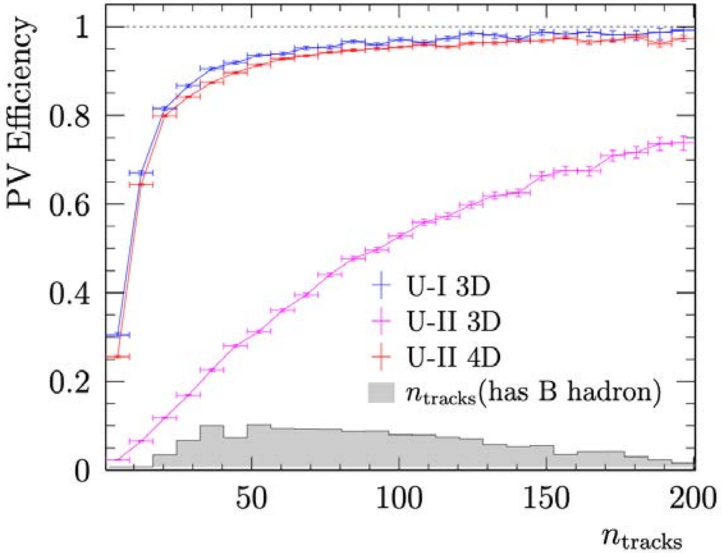

Reconstruction efficiency vs the number of tracks per primary vertex, comparing the Upgrade I 3D reconstruction in both data conditions, and a variant using timing information to resolve the primary vertices

4D pixel:
A solid state pixel sensor (pitch ≈ 50 μm) bearing time information

Track merging: bad Primary (and Secondary) Vertex reconstruction

Incorrect PV assigned to tracks: poorly measured lifetime (dominant sistematic effect for time-dependent analysis)

PV reconstruction efficiency as as function of the single hit resolution, for all vertices (left) and for vertices where at least one of the decay products is a charm hadron (right).

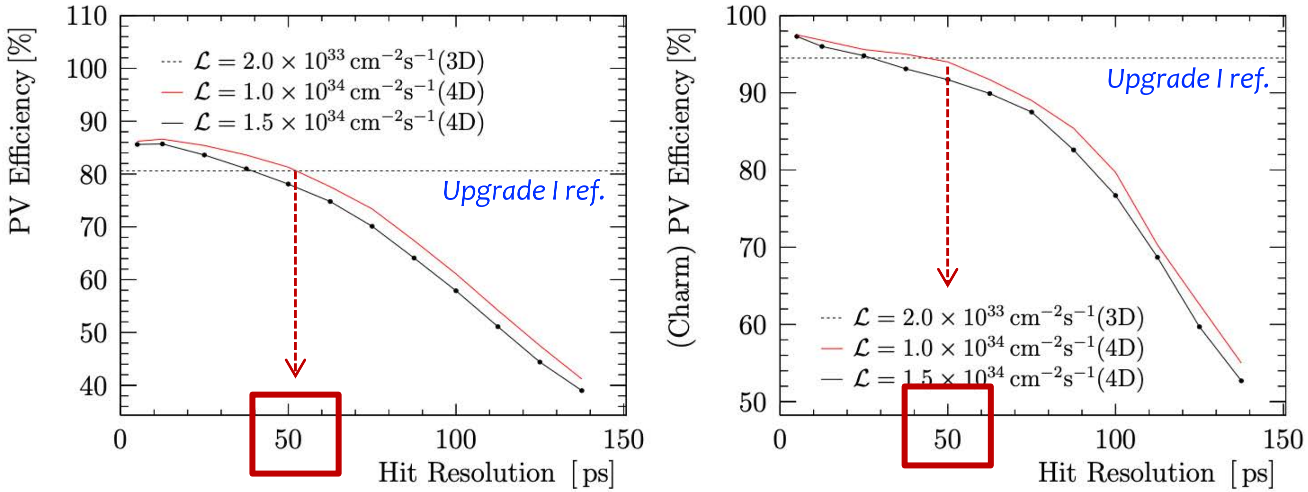

50 ps per hit (corresponding to 20 ps per track) are sufficient to recover the Upgrade-I efficiency

Outline

- **Basics** on fast timing and 4D pixels (pixels with timing)
- An example: LGADs
- Fast timing with «**Geometric**» (or 3D silicon sensors) and their design
- Developed **tools for the design and modeling** of 3D silicon sensors
- Characterization and **performance** of 3D silicon sensors on timing
- Use of **software tools for the accurate interpretation** of the experimental results
- **More results** on 3D silicon sensors

Timing fundamentals

… in 3 slides (1)

Good timing is all about limiting both statistical and sistematic uncertainties in measuring the signal Time-of-Arrival (ToA), that is, a voltage signal threshold-crossing time

minimizing σ_t

$$\boxed{\sigma_{ej} = \frac{\sigma_V}{\left.\frac{dV}{dt}\right|_{V_T}}}$$

statistical — pseudostatistical — Digitization error

$$\sigma^2_t = \sigma^2_{ej} + \sigma^2_{\delta\text{-}ray} + \sigma^2_{un} + \sigma^2_{TW} + \sigma^2_{TDC}$$

sistematic

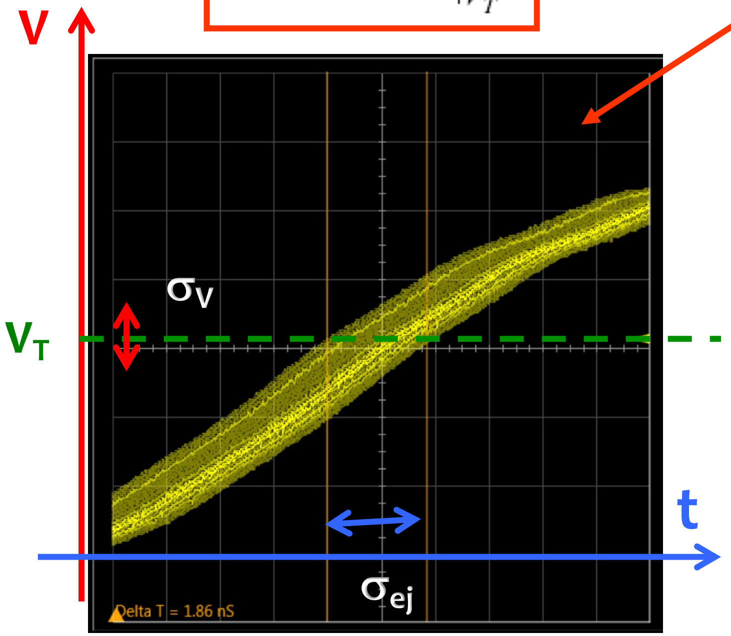

Effect of intrinsic electronic noise on time purely statistical

aka Landau noise, effect of out-of-time secondary ionization (knock-on electrons)
Physical limit in planar sensors

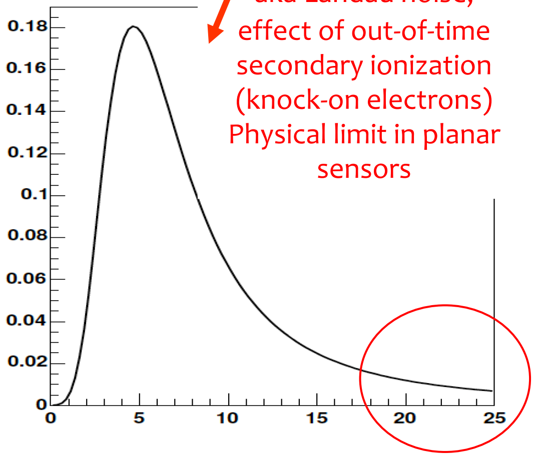

Landau amplitude distribution

Differences in the signal shapes due to uneveness in the E field across the sensor volume

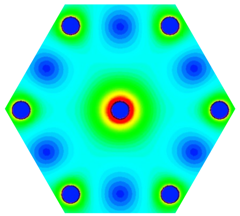

E field map in a hexagonal 3D pixel (see next slides)

Time walk: dependence of the crossing time on the signal amplitude
Can be back-corrected once the amplitude is known

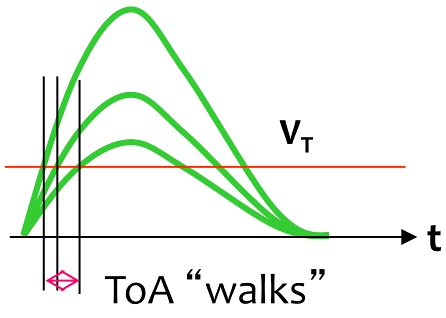

Unavoidable digitization error in time-to-digital conversion
Can be strongly (but not completely) reduced

Timing fundamentals

…in 3 slides (2): σ_{ej} (aka σ_j)

The main contributions to σ_t, which we must optimise, remain σ_{ej} and σ_{un}

Electronic jitter

$$\boxed{\sigma_{ej} = \frac{\sigma_V}{\left.\frac{dV}{dt}\right|_{V_T}}} \approx \frac{\sigma_V}{S/t_r} = t_r\,(S/n)^{-1}$$

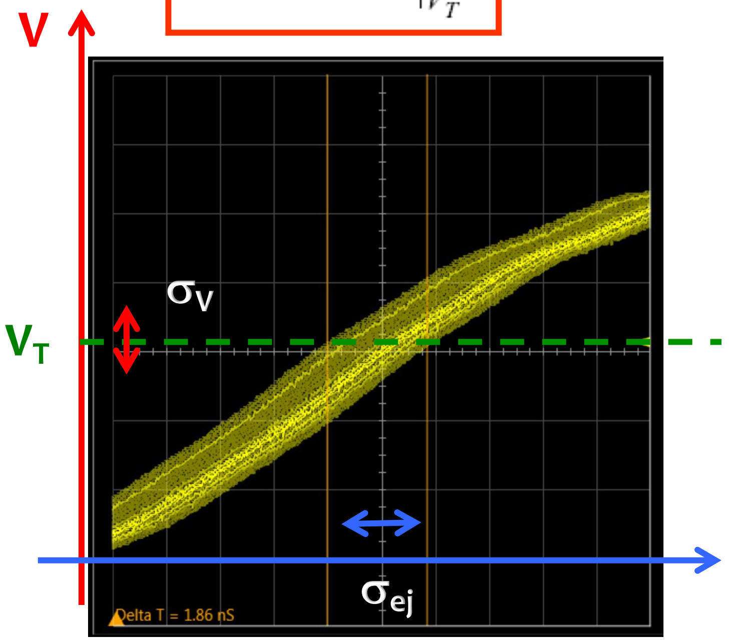

Effect of intrinsic electronic noise on time

Purely statistical

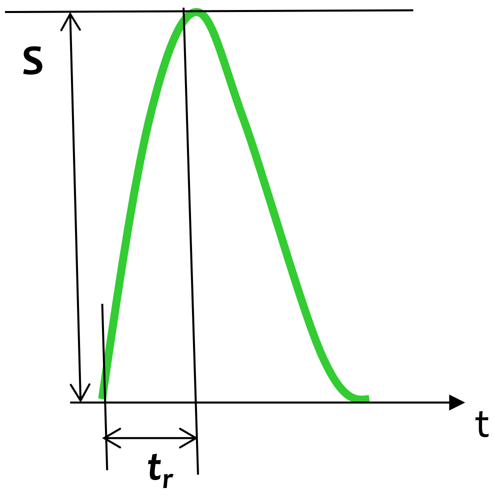

We need:

1. **Short rise time t_r (high F/E amplifier slew rate)**
2. **Low voltage noise *n***
3. **High signal amplitude S**

Remarks:

- **Requirements #1 and #2 are competitive.** They depend mainly on the FE performance/characteristics and on sensor capacitance (small is better)
- **Requirement #3 depends mainly on the amplifier** (Gain and BW) but also on the **amount of charge delivered** at the electrodes by the sensor: a minimum sensor thickness is necessary to deliver **enough charge by dE/dx**

Timing fundamentals

… in 3 slides (3): σ_{un} (aka σ_{dis}, σ_{wf})

The native signal on the pixel electrodes (before the necessary FE processing) is a current signal (i), induced by the movement of the ionization-freed charge carriers (e/h), under the action of the electric field E. The induced current contribution in each point of the sensor volume is given by the Ramo theorem (E_w is the weighting field*):

$$\boxed{\boldsymbol{i} = q\boldsymbol{E}_w \cdot \boldsymbol{v}}$$ → High and uniform E field

→ Uniform E_w to have uniform signal shapes (smaller dipersion).
→ Carrier velocities v strictly depends on the electric field E. Increasing E, they tend to be saturated and equalized, that is more uniform.

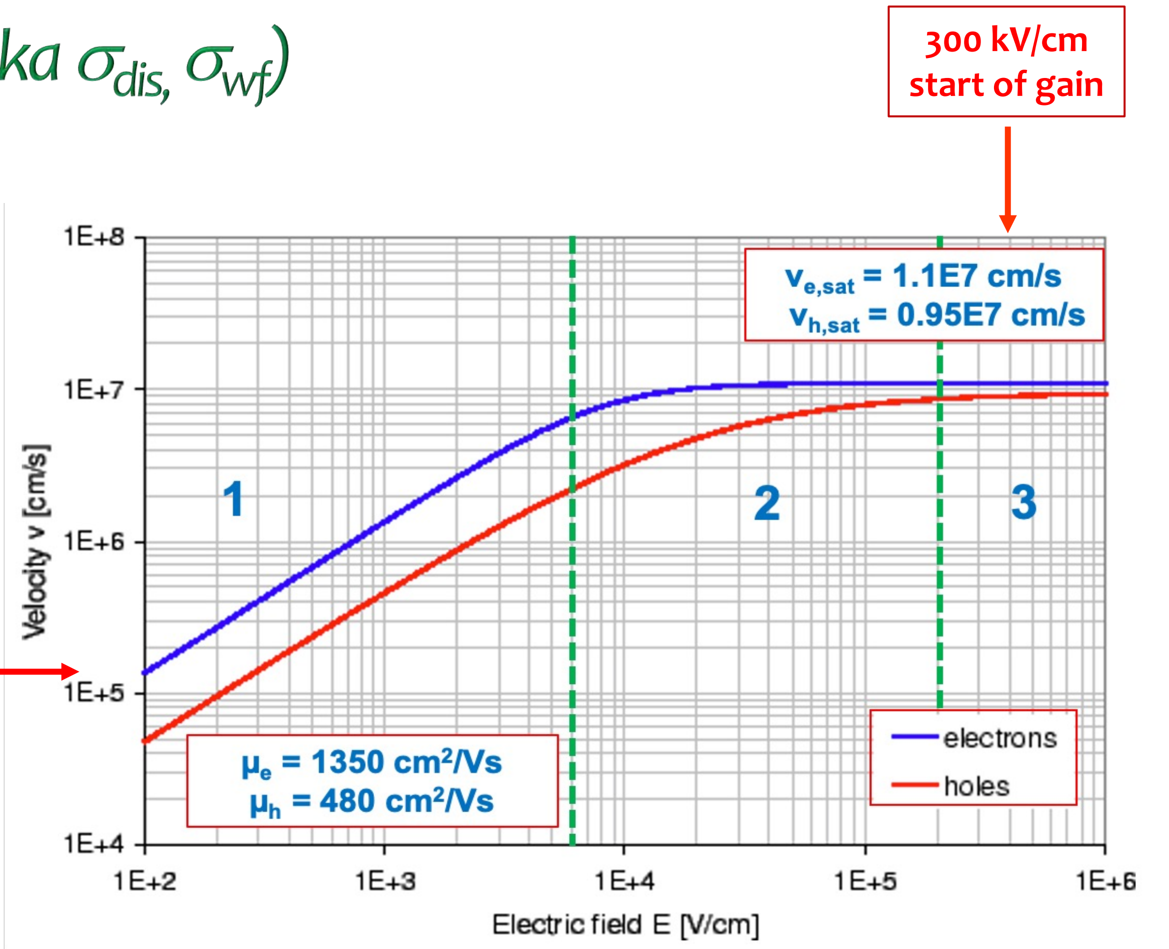

Carrier velocities vs electric field in silicon:
1) Low-field regime (v= μE);
2) Transition regime;
3) Saturation regime

Remarks:

- Uniformity of E and E_w comes from the pixel geometry and prediliges a parallel-plate electrode shape (low dispersion is better than speed), where $E_w = 1/d$ (d = inter-electrode distance)
- Small d gives higher current and shorter charge collection times (but also higher capacitance: trade-off)

*E_w: E field in absence of the moving charge, collecting electrode put to voltage = 1 V, and all other electrodes grounded

Summary on «timing fundamentals»

- A (timing) tracking system detects Minimum Ionizing Particles
- Uncertainties in the measurement of the Time-of-Arrival of the signal are statistical and sistematic. The latter can be strongly mitigated if the relavant information is acquired (e.g. signal amplitude) with well-known techniques (es CFD).
- The main and more troublesome contributions to ToA uncertanties are the electronic jitter, due to the voltage noise, and the field uneveness inside the pixel, which causes important variation in the induced signal shapes (→ time dispersion).
- The triple gem of high time resolution is:
  1. High S/n ratio → enough primary charge (enough dE/dx thickness)
  2. Short signal rise time → high F/E BW, short charge collection time (small inter-electrode distance d)
  3. Uniform field → parallel-plate geometries ($E_w \approx 1/d$)
- The current signal shape at the electrodes depends on the E_w field inside the pixel, so for example on d. Small d detectors generate faster and higher current signals. Furthermore, a small d limits the length of the signals (Charge Collection Time), which is beneficial for fast timing
- Front-end electronics is absolutely decisive for the final timing performance

(not so) «Side» Effects in 4D Timing

When 4D timing (pixel with timing) is concerned, we should **NEVER NEGLECT** the following mandatory additional requirements:

1. High luminosity implies high intensities of interactions and therefore high fluences (for sensors) and high doses (for electronics). In the inner regions of the apparatus, numbers are close to fluences $\Phi = 10^{17}$ 1 MeV n_{eq}/cm^2 and > 2 Grad
2. A detection efficiency of $\varepsilon > 99\%$ per layer is tipically required (high fill factor)
3. Material budget must be kept below 1 and 0.5 % radiation length per layer
4. Very challenging front-end electronics must be developed. Today a complete solution for that is FAR from being available.

source:
Considerations for the VELO detector at the LHCb upgrade II – CERN-LHCb-2022-001

Requirement	scenario S_A	scenario S_B
Pixel pitch [µm]	≤ 55	≤ 42
Lifetime fluence [1×10^{16} 1 MeV n_{eq}/cm^2]	> 6	> 1
TID lifetime [MGy]	> 28	> 5
Sensor Timestamp per hit [ps]	≤ 35*	≤ 35
ASIC Timestamp per hit [ps]	≤ 35*	≤ 35
Hit Efficiency [%]	≥ 99	≥ 99
Power per pixel [µW]	≤ 23	≤ 14
Pixel rate hottest pixel [kHz]	> 350**	> 40
Max discharge time [ns]	< 29	< 250
Bandwidth per ASIC of 2 cm^2 [Gb/s]	> 250	> 94
Material budget	$\leq 0.8\%$ X_0 per station (all included)	

… and what is more important:
All the above requirements must be met at the same time, along with high time resolution !!!

Low Gain Avalanche Diodes

Go thin and add gain !

Reduce thickness (to 50 – 35 μm) for fast collection time.
Add gain by doping layer to recover and get higher signal

MM Obertino – INFN Torino

High electric field accelerates e- enough to start multiplication

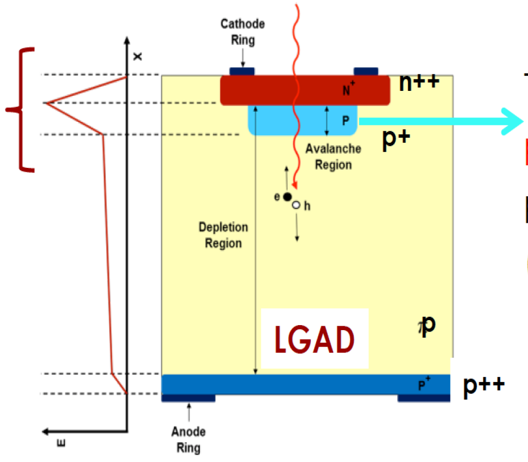

Thin, highly doped, p-implant near the p-n junction ($N_d \sim 10^{16}$ Boron/cm^3)

Low gain ≈ 5-10

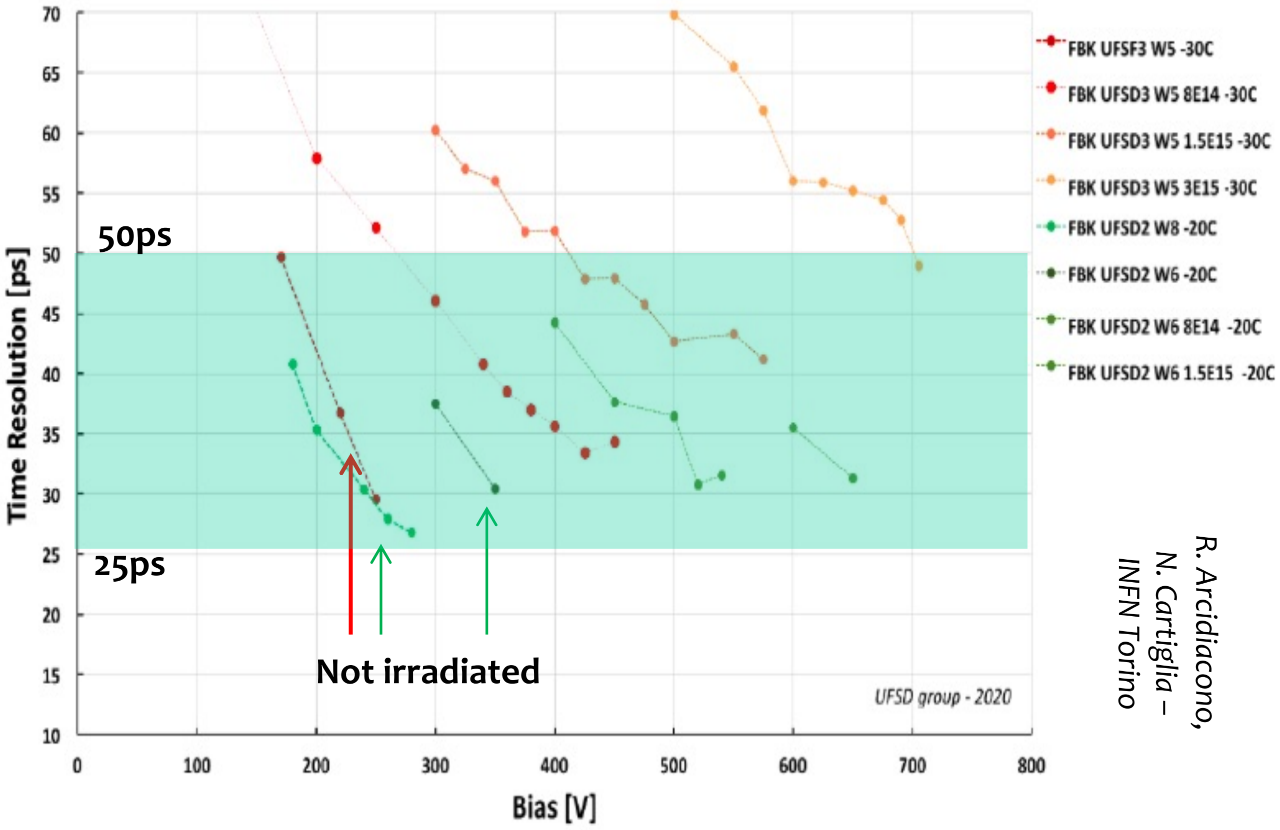

R. Arcidiacono, N. Cartiglia – INFN Torino

Great advantage: excellent time resolution, standard/easily accessible planar technology → several vendors, lower costs

Open issues:

1. Small pitch is difficult (the need of pixel isolation lowers the fill factor: developments on Trench-LGAD, AC-LGAD, Inverted-LGAD).
2. Radiation “eats” the Boron and cancels the gain effect around 10^{15} n_{eq}/cm^2

R&D: B → Ga, C... (heavier dopants)

Improvement by ≈ x3 – x4

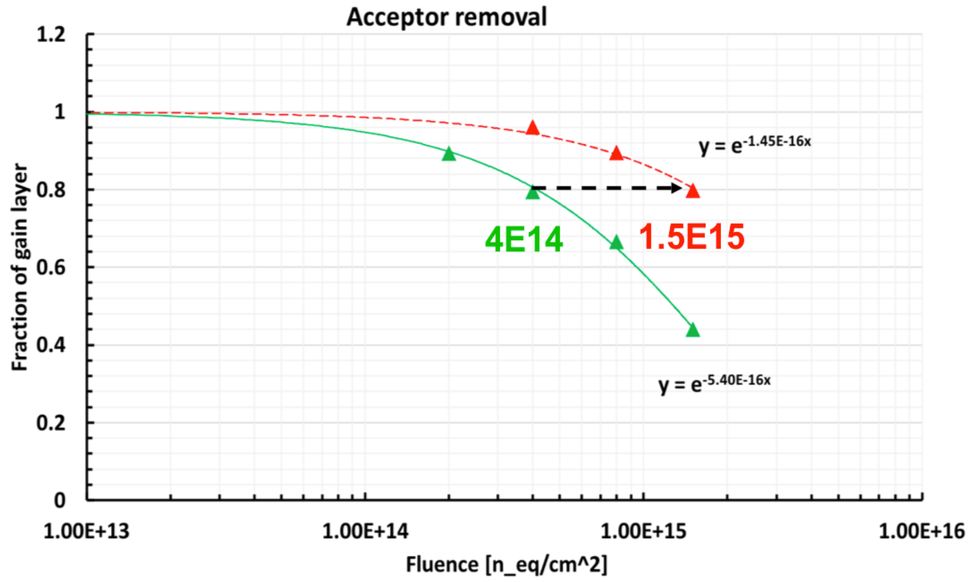

A different approach: 3D silicon sensors

Go… Geometric !

Concept (S. Parker et al., 1997):
Perpendicular electrodes make
Inter-electrode distance d
independent of sensor thickness z

Sensitive volume and electrode shapes can be designed and modeled for maximum performance

High and uniform E field

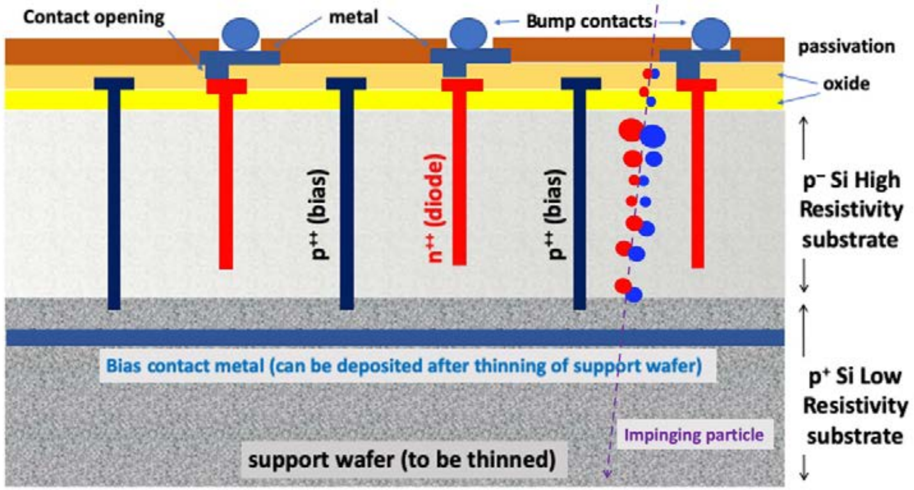

Deep Reactive Ion Etching
(MEMS technology)

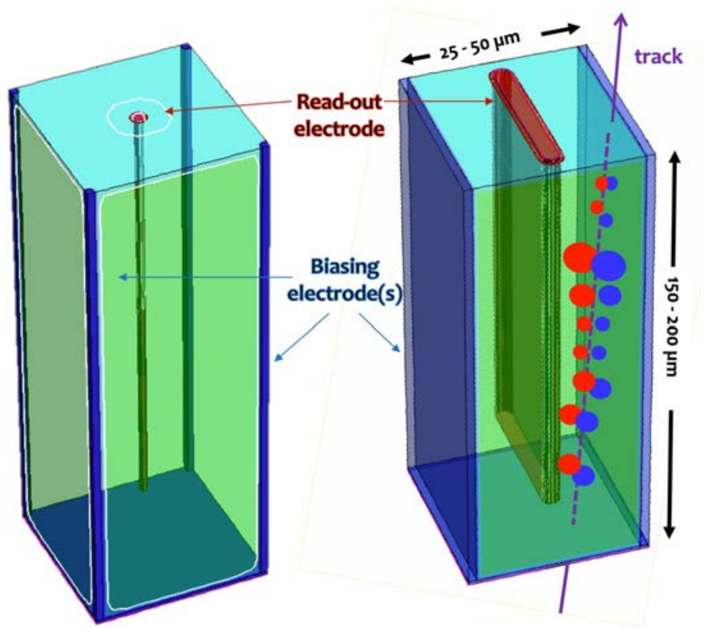

columns trenches

Column or trench aspect ratio ≈ 30:1

$$\boldsymbol{i} = q\boldsymbol{E}_{W} \cdot \boldsymbol{v}$$

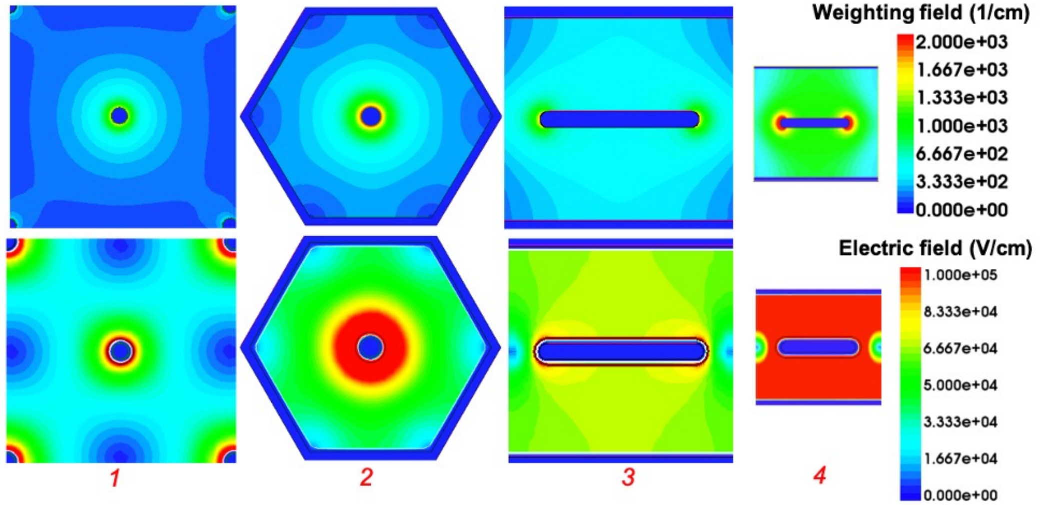

TCAD Sentaurus output: 2D model simulation of three different electrode geometries at bias voltage $V_{bias} = -100$ V

Geometric playgound (TCAD Sentaurus)
Technology CAD by SYNOPSYS®

- TCAD is a software dedicated mainly to µ-electronics technology definition and design

- We use it to estabilish
  1. the sensor detailed structure (geometry, materials, doping)
  2. electric and weighting field detailed maps,
  3. velocity maps

- The calculated output values are defined on a mesh, defined by the user. The mesh definition is critical in the development of the simulation

- Each mesh element is assigned a tensorial list of values, defining the relevant variables (3D position, fields, velocities) of the model

- TCAD allows also injecting charge deposits in specific points of the volume but not according to physics-based simulation models

- TCAD can also calculate the carrier transport mechanisms but in a very inefficient way (charge cloud transport)

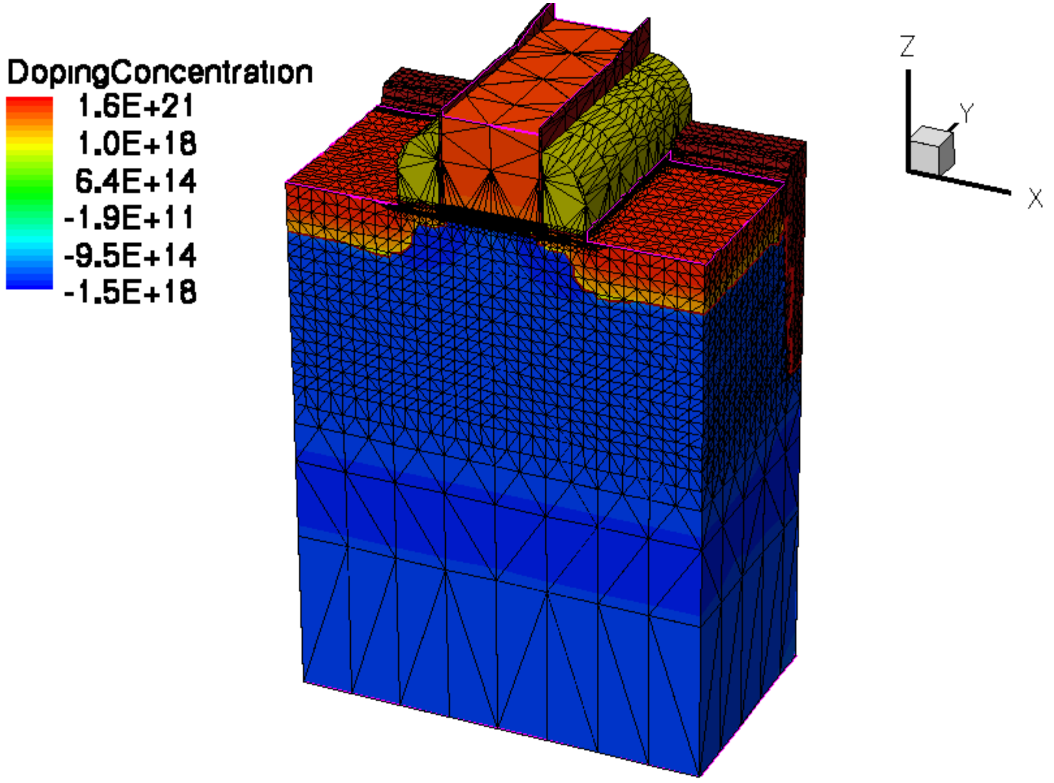

A CMOS transistor in TCAD, with highlighted tensorial mesh grid.

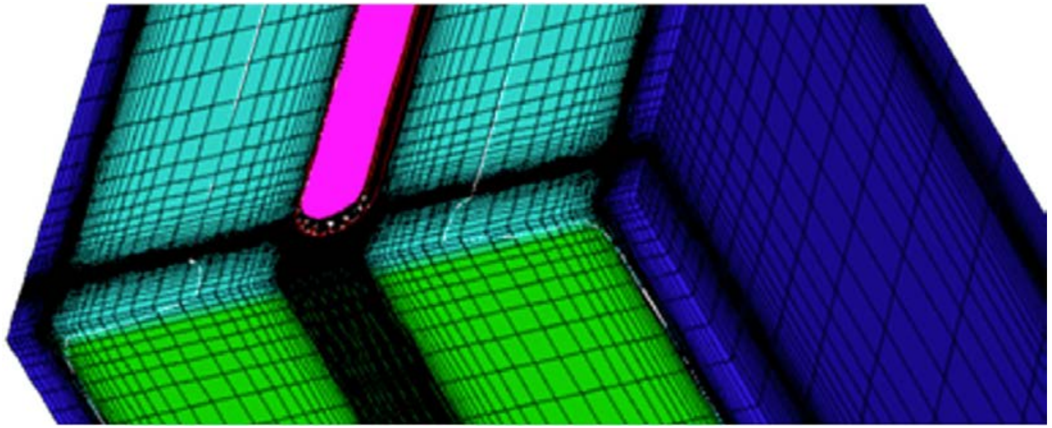

3D-silicon sensor with highlighted tensorial mesh grid.

The playgound and the game

CCT and current signals

https://github.com/MultithreadCorner/Tcode

GPL3 license

The TCoDe simulation flow

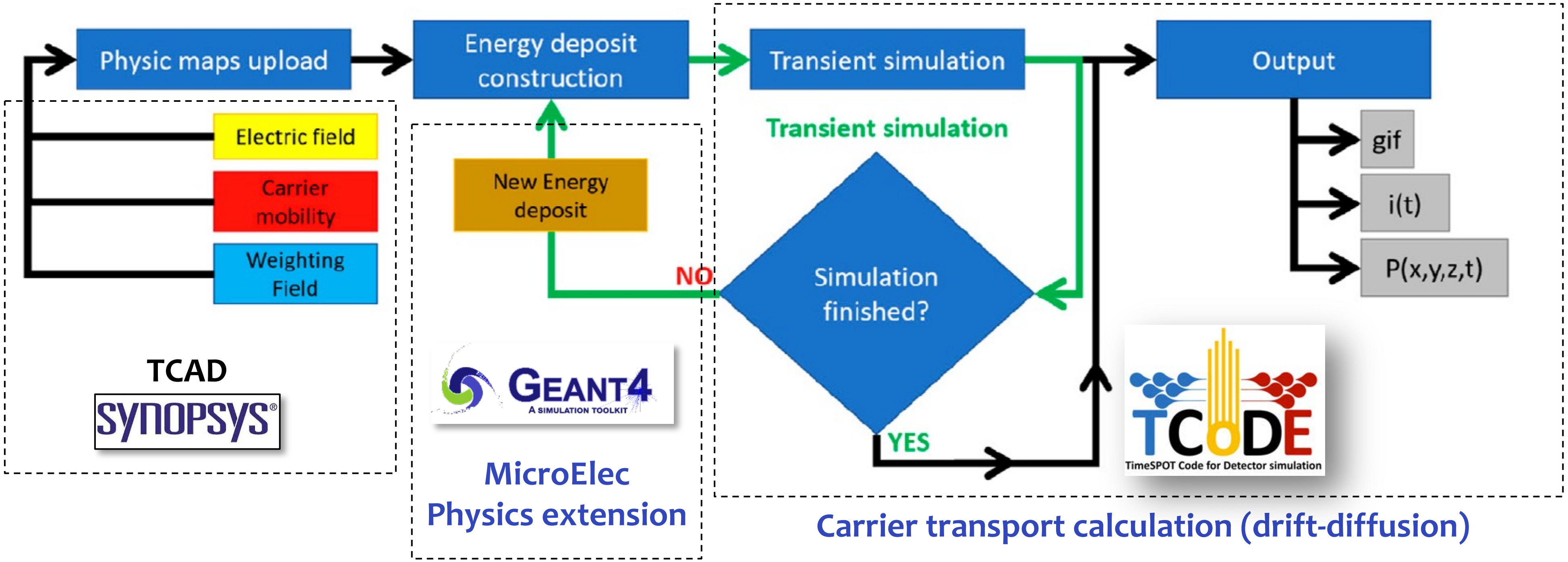

The carrier motion calculated using a 4th-order Runge–Kutta algorithm and the thermal diffusion equation.
The contribution of each carrier to the current induced on the readout electrode is determined with the Ramo theorem for each time interval.
Multi-threaded approach (Hydra libraries): each carrier is followed independently in a separate computing thread, either in CPU or GPU.

Brundu D, et al. (2022) Modeling of Solid State Detectors Using Advanced Multi-Threading: The TCoDe and TFBoost Simulation Packages. Front. Phys. 10:804752.
Loi A, Contu A, Lai A. Timing Optimisation and Analysis in the Design of 3d Silicon Sensors: the TCoDe Simulator. J Inst (2021) 16:P02011

TCoDe:

Geant4 deposit take life!

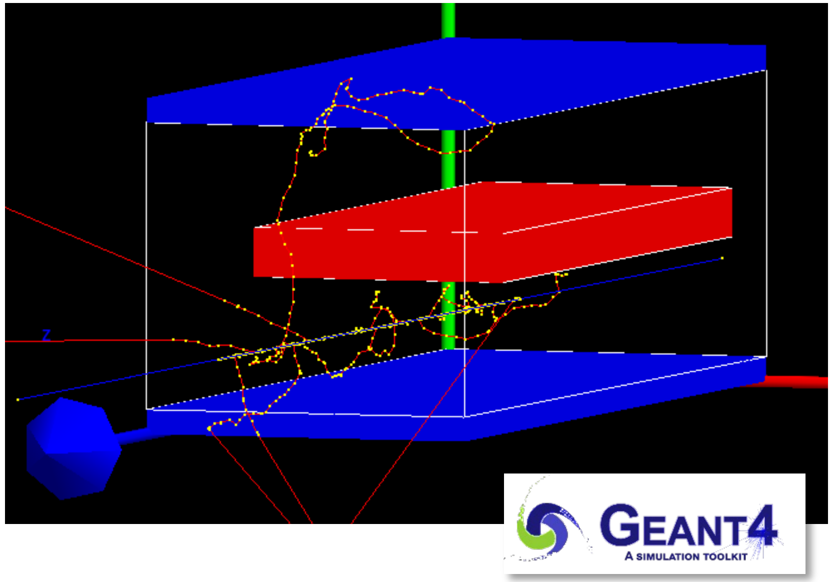

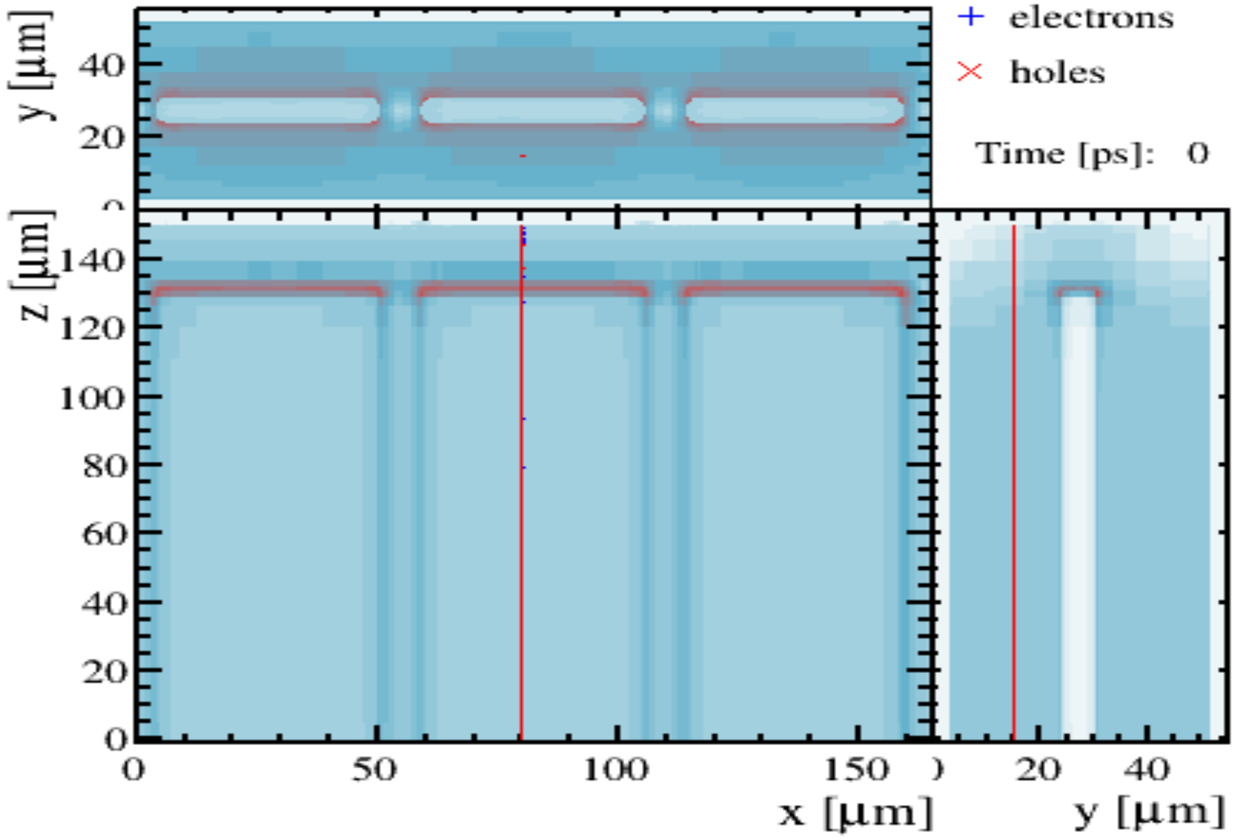

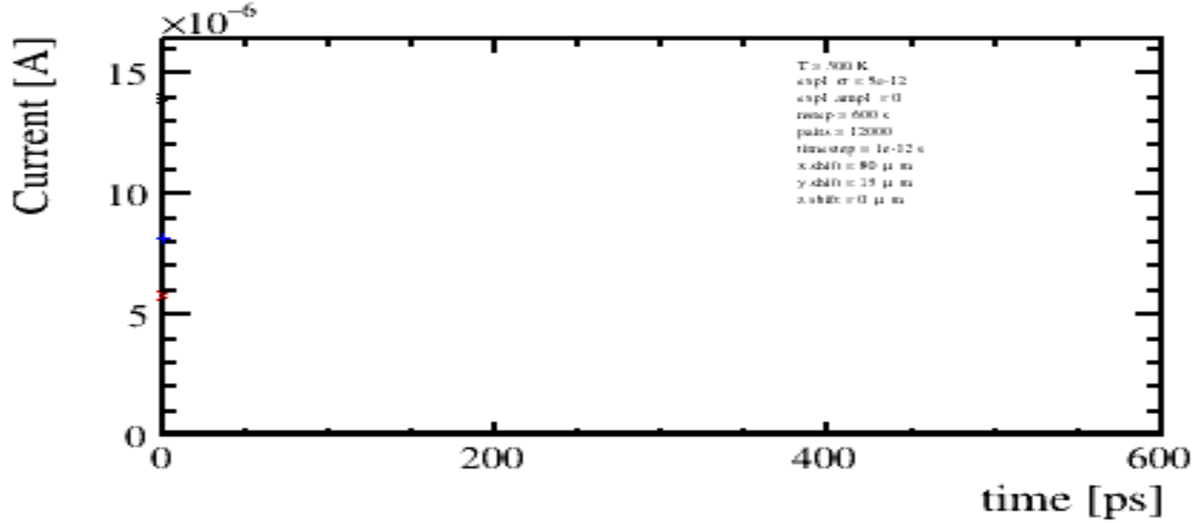

Energy deposits

Geant4 and/or analytic

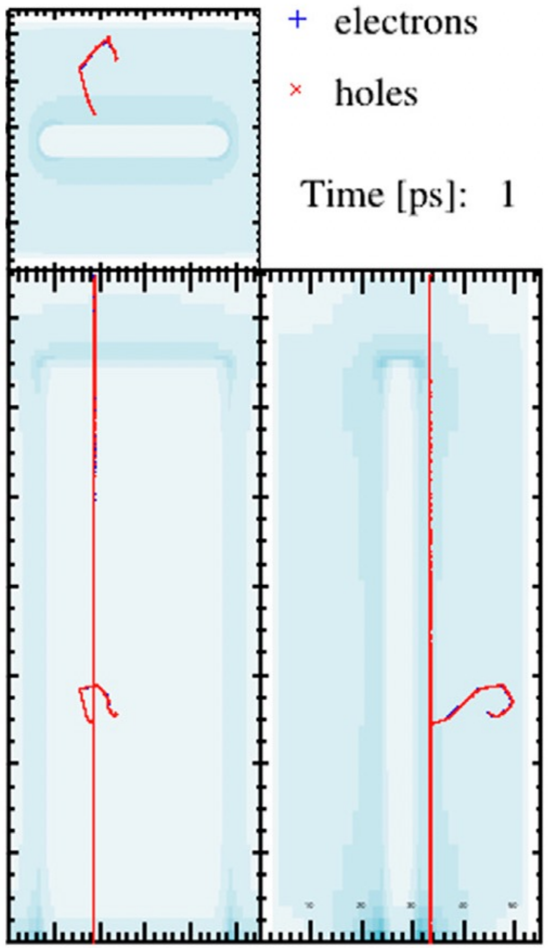

MIP deposit shape

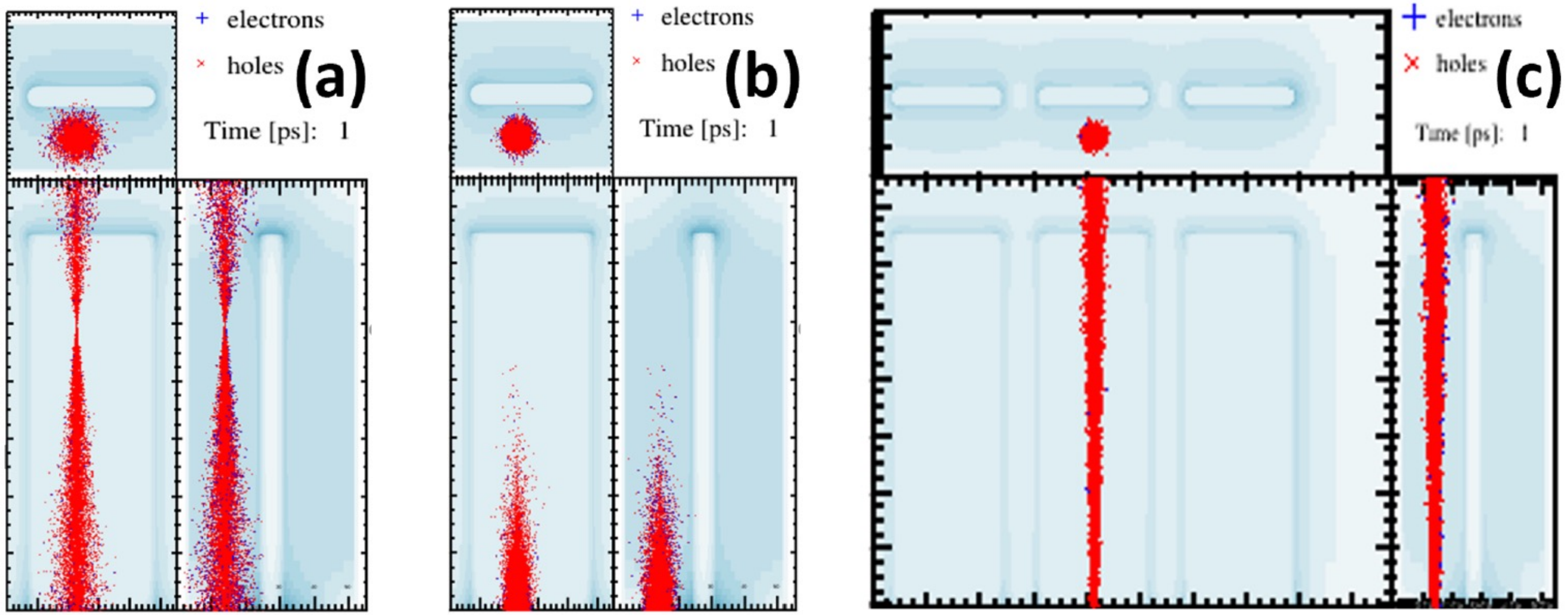

Examples of calculated energy deposit shapes **from laser sources** inside a TimeSPOT 3D-trench structure:

(a) Deposit with focus inside the active bulk.
(b) Deposit shape due to high absorption (655 nm wavelength)
(c) Deposit of IR laser source (1030 nm wavelength), emulating a MIP.

Time resolution: laser-emulated MIP studies

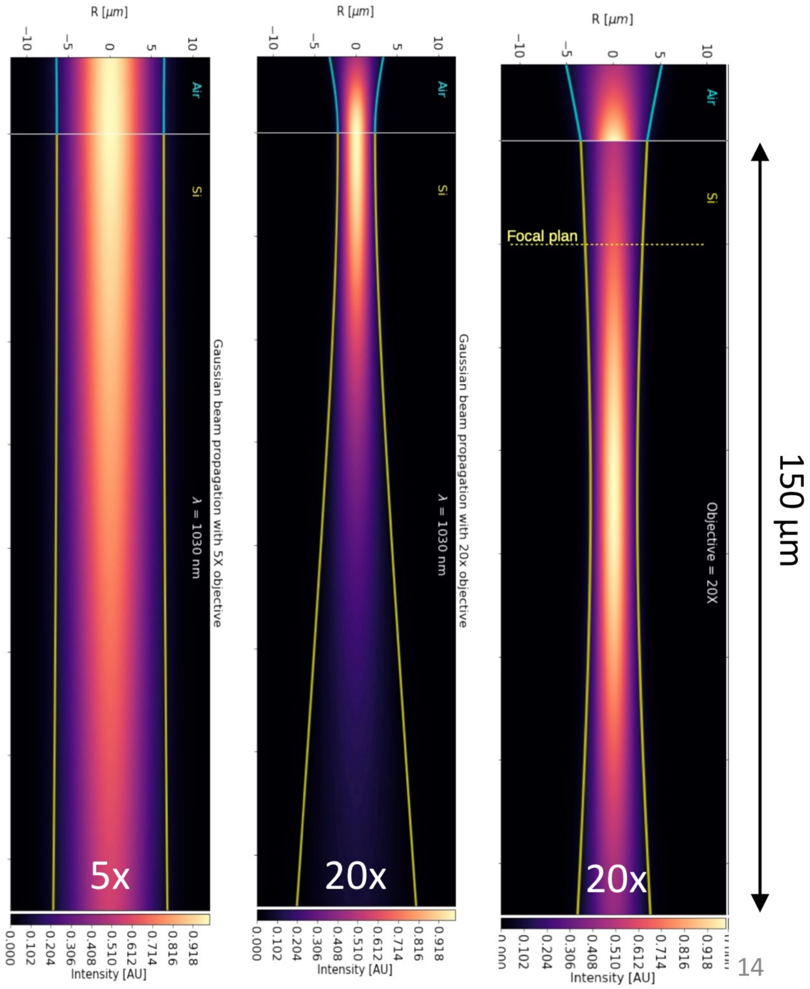

Pulsed laser:

- IR Laser (1030 nm), FWHM < 200 fs
- Optical fiber from laser to microscope.
- Focused spot of ~ 5 μm
- Observation camera
- XY closed loop stages
- Optical laser time reference: accuracy <1ps using TimeSPOT sensors, custom Si-Ge F/E and 10 MIP-equivalent pulse

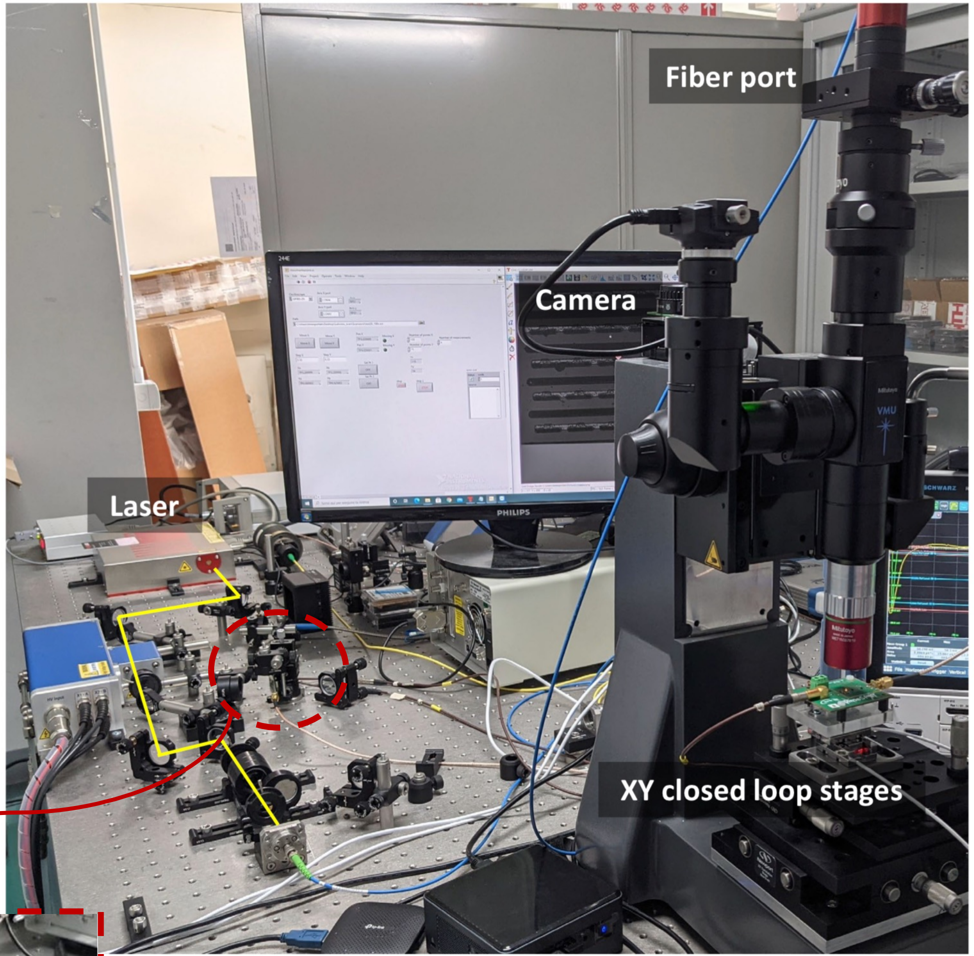

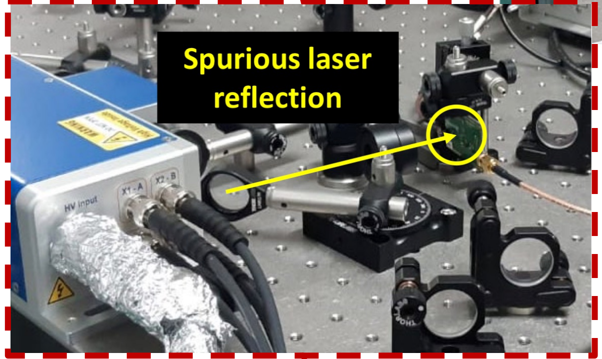

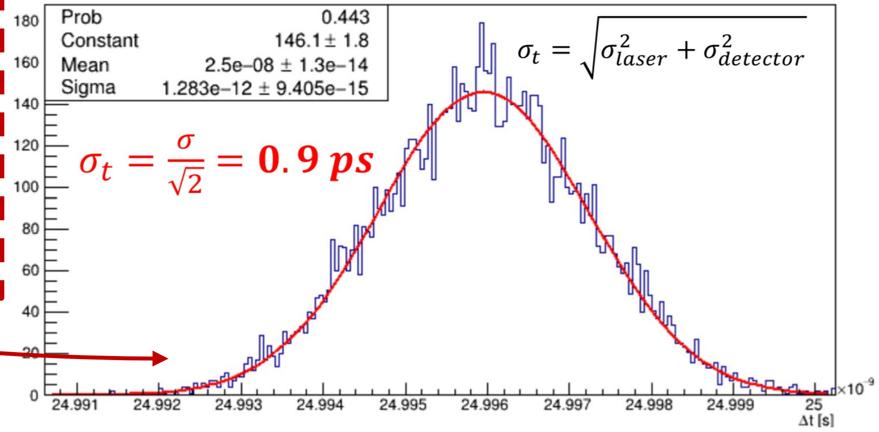

By choosing the waist shape (changing optics) and properly calibrating the laser intensity (using a precision CSA) a MIP-like deposit is generated

Comparison of TCoDe vs TCAD outputs

Induced current signal

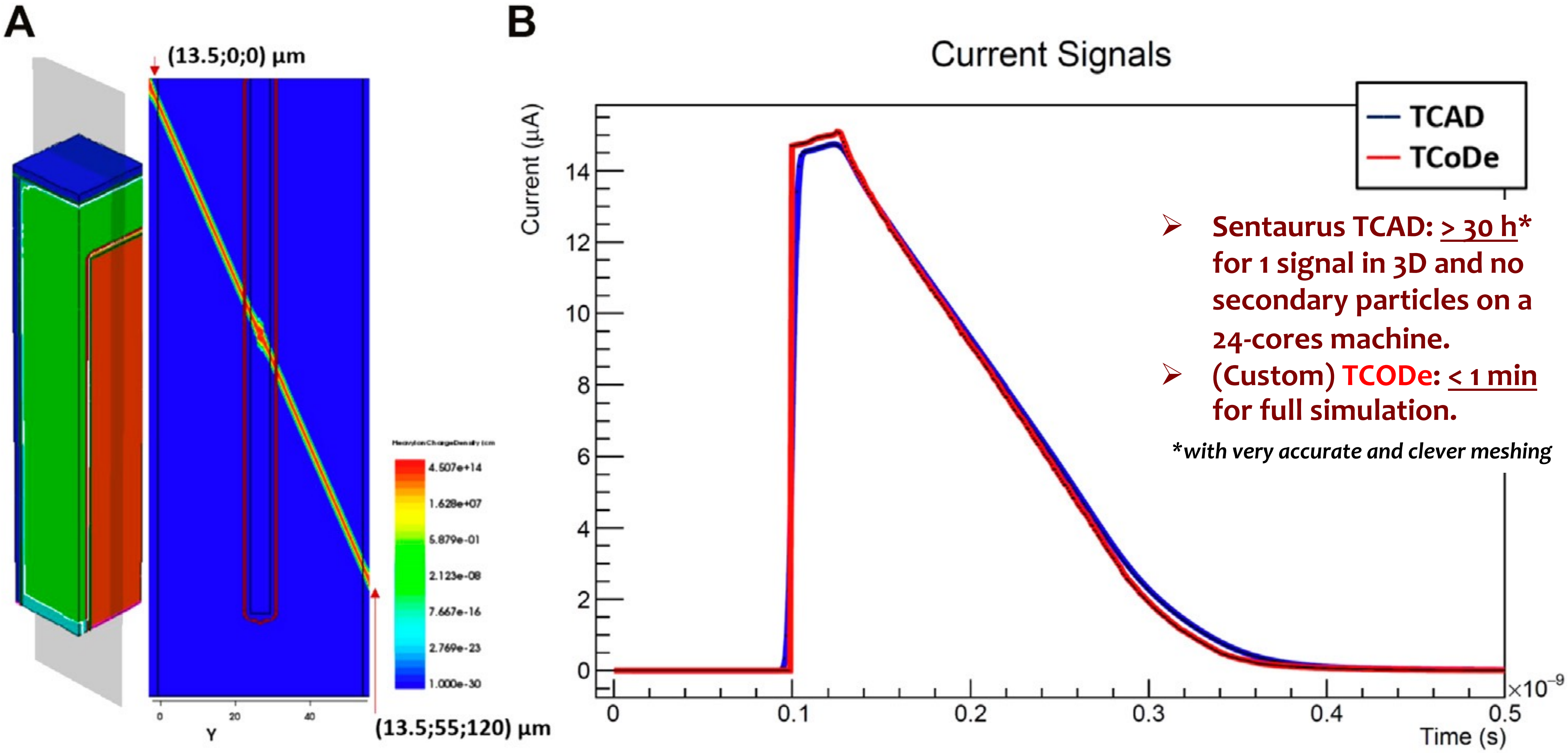

- **Sentaurus TCAD: <u>> 30 h</u>* for 1 signal in 3D and no secondary particles on a 24-cores machine.**
- **(Custom) TCODe: <u>< 1 min</u> for full simulation.**

****with very accurate and clever meshing***

Brundu D, et al. (2022) Modeling of Solid State Detectors Using Advanced Multi-Threading: The TCoDe and TFBoost Simulation Packages. Front. Phys. 10:804752.

Loi A, Contu A, Lai A. Timing Optimisation and Analysis in the Design of 3d Silicon Sensors: the TCoDe Simulator. J Inst (2021) 16:P02011

TCoDe operation and statistics

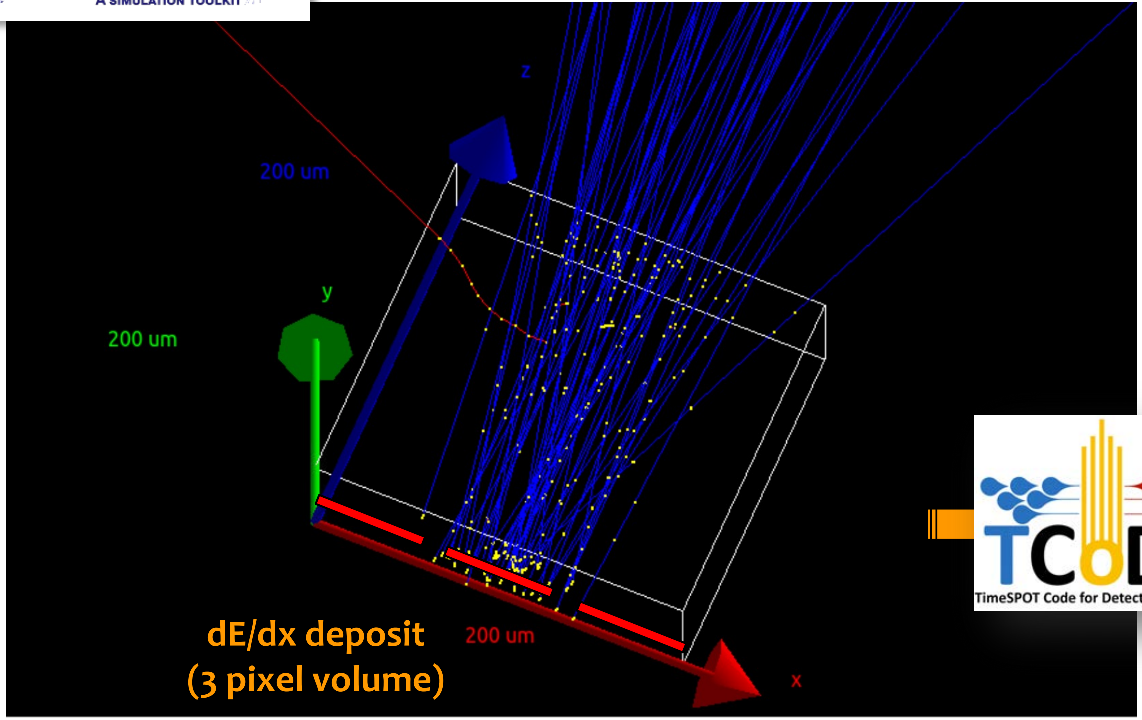

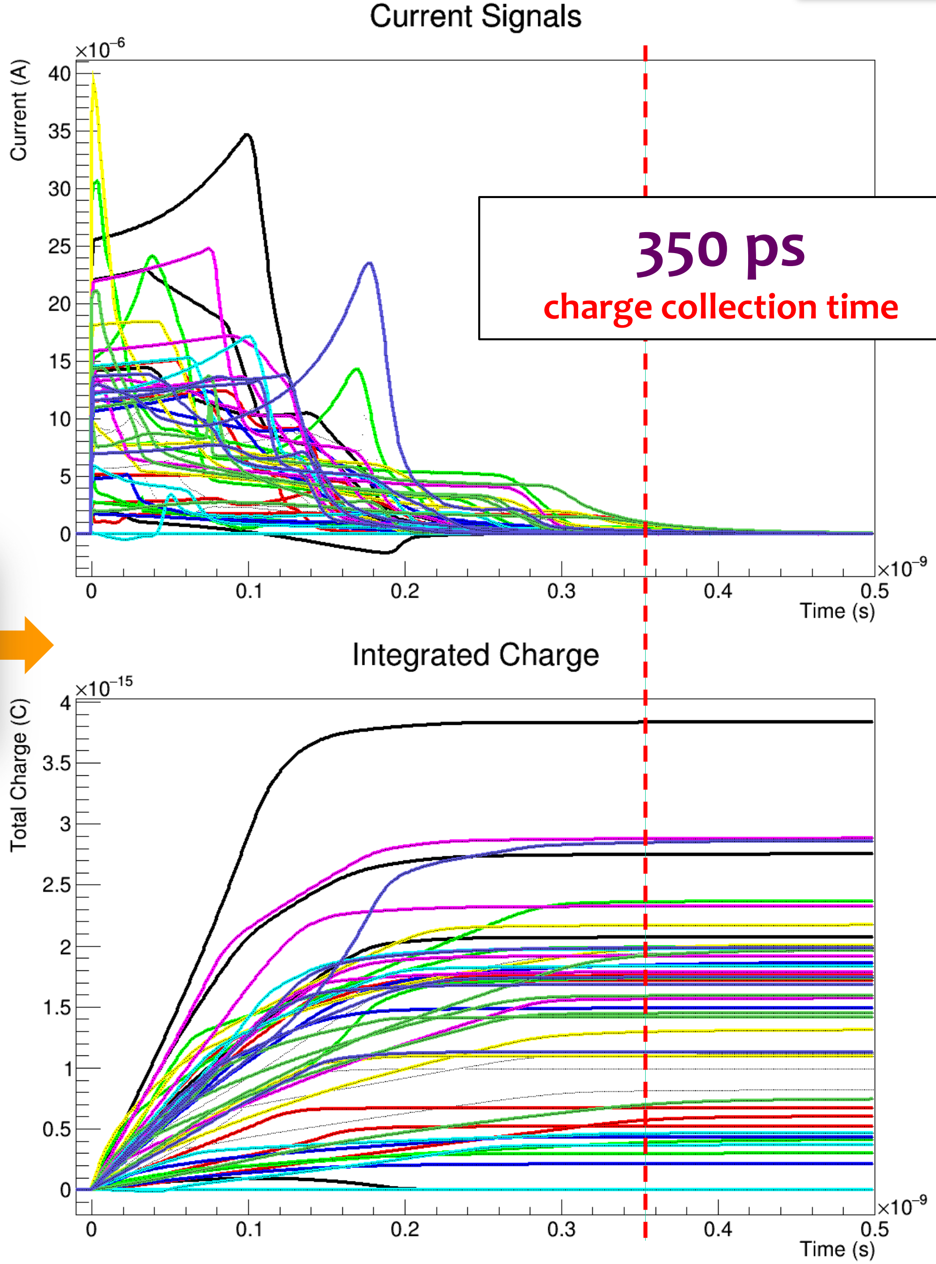

350 ps
charge collection time

50 tracks
Induced current signals calculated by TCODE
(input to F/E electronics model)
1h40' in ST (Intel®Xeon®CPU X5450 – 10 GB RAM)
1'40" on a gaming laptop in MT
2-3 months on TCAD (estimate)

A. Contu, A. Loi – INFN Cagliari

Charge Collection Time

Curves and maps

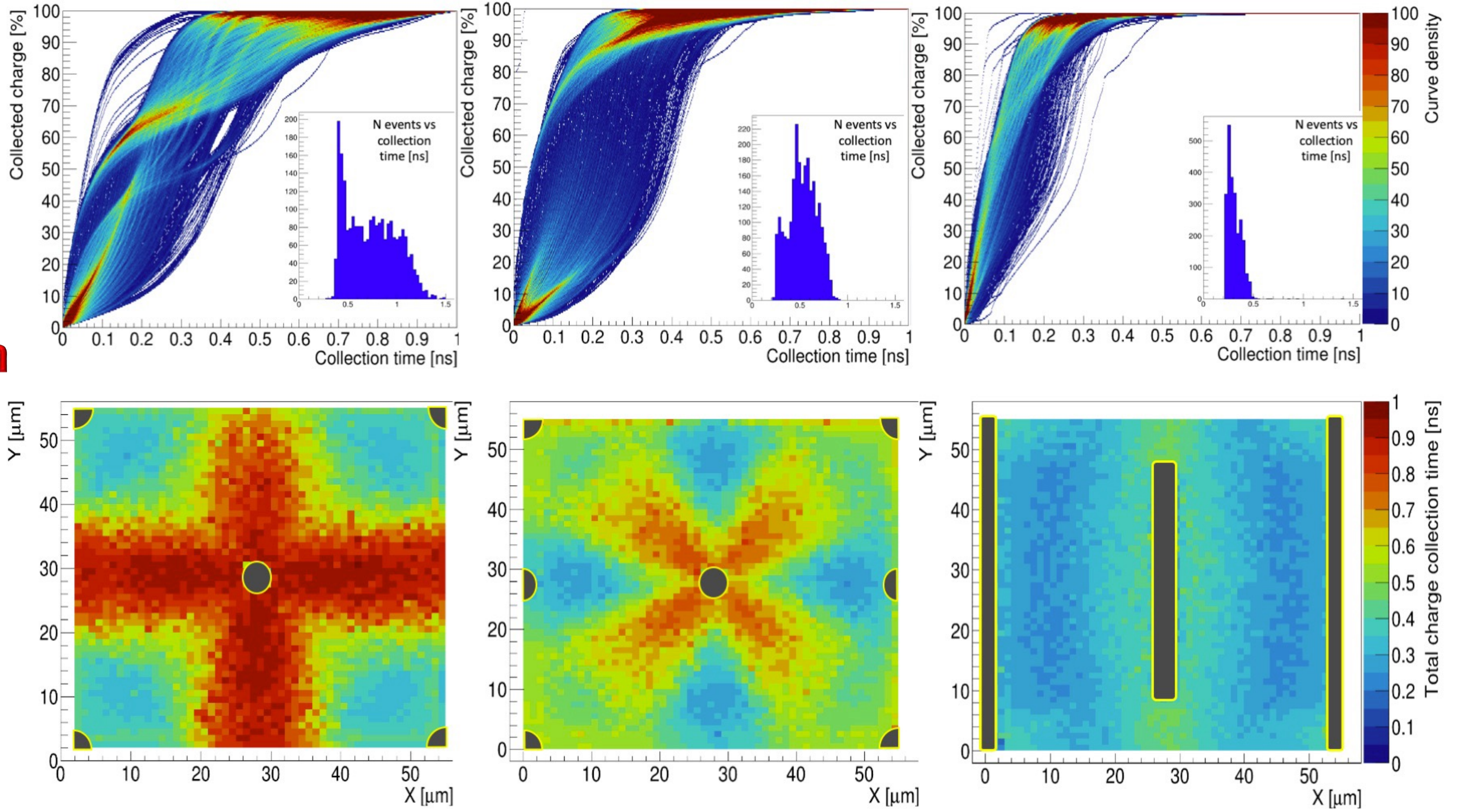

Time performance comparison among three different 3D geometries at V_{bias} = –100V (from left to right: five columns, nine columns and trench geometry). (Top) percentage of total charge collected on the electrodes versus time. (Top inserts) distribution of charge collection time for the three geometries. (Bottom) time for complete charge collection versus impact point for the same geometries. Each simulation is based on about 3 000 MIP tracks.

The best geometry for timing
3D-trench silicon pixel

- **55 μm pitch** for compatibility with Timepix family ASICs
- **150 μm thickness** for enough primary charge by dE/dx (2 fC), while keeping a good trench aspect-ratio and low material budget

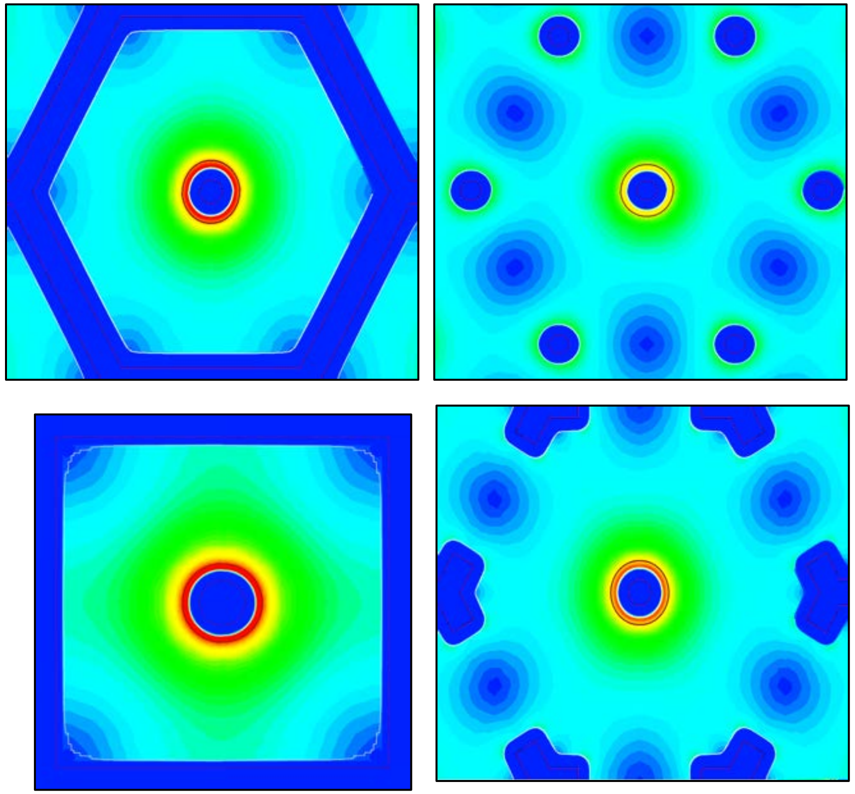

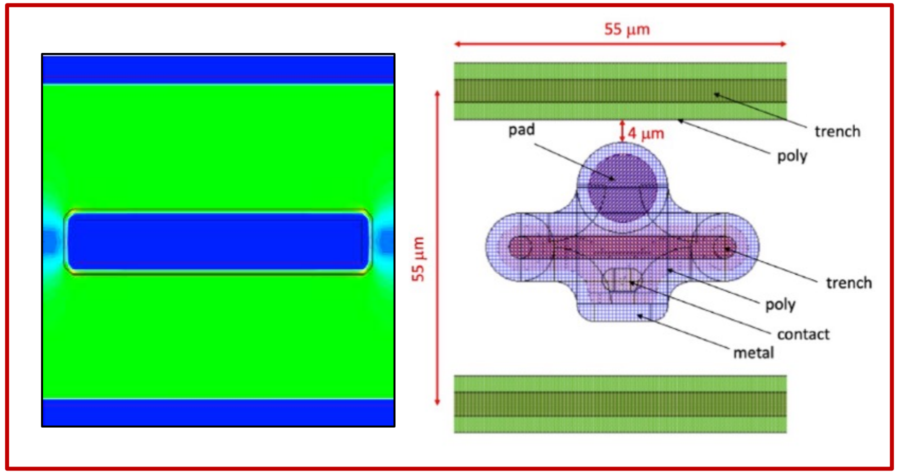

layout

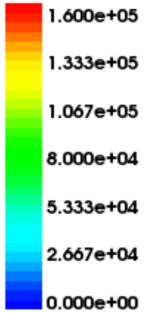

−100 V bias
300 K temperature

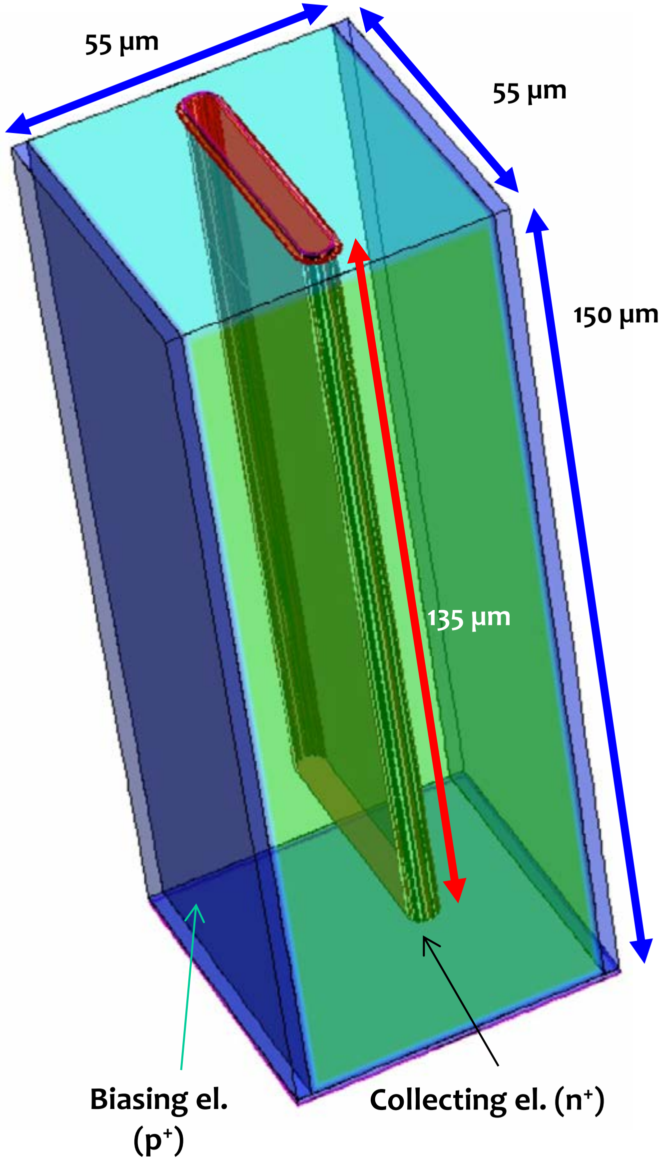

Sensor fabrication @ FBK

2 batches (2019 and 2020)

temp metal
for static tests

Matrix of 3D-trench sensors

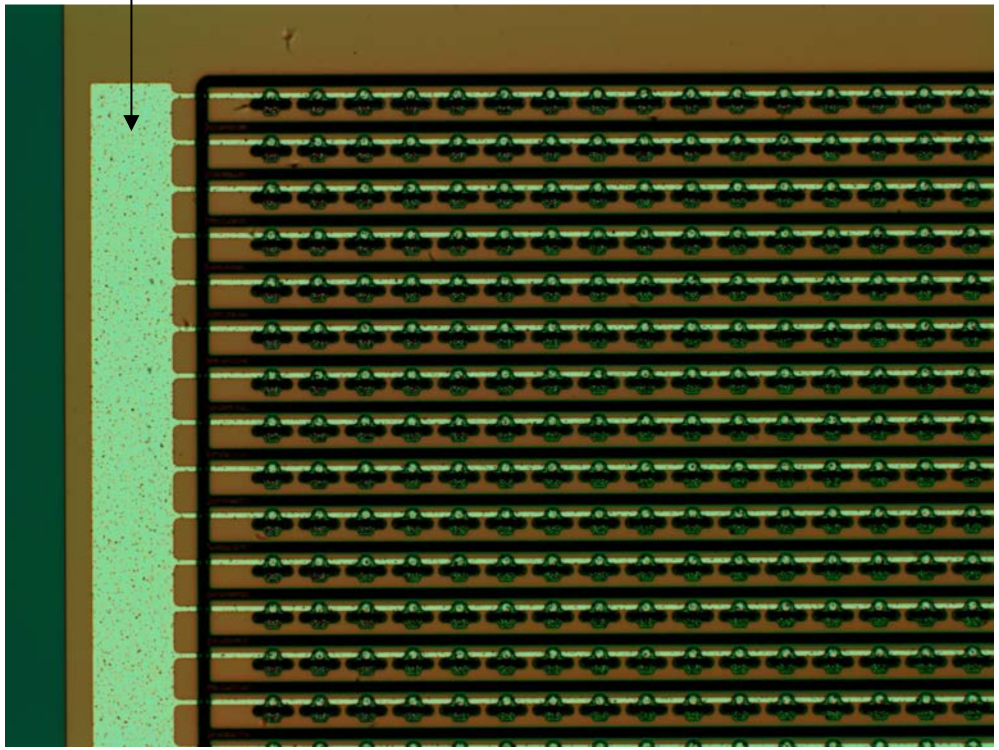

collecting trench

bias trench

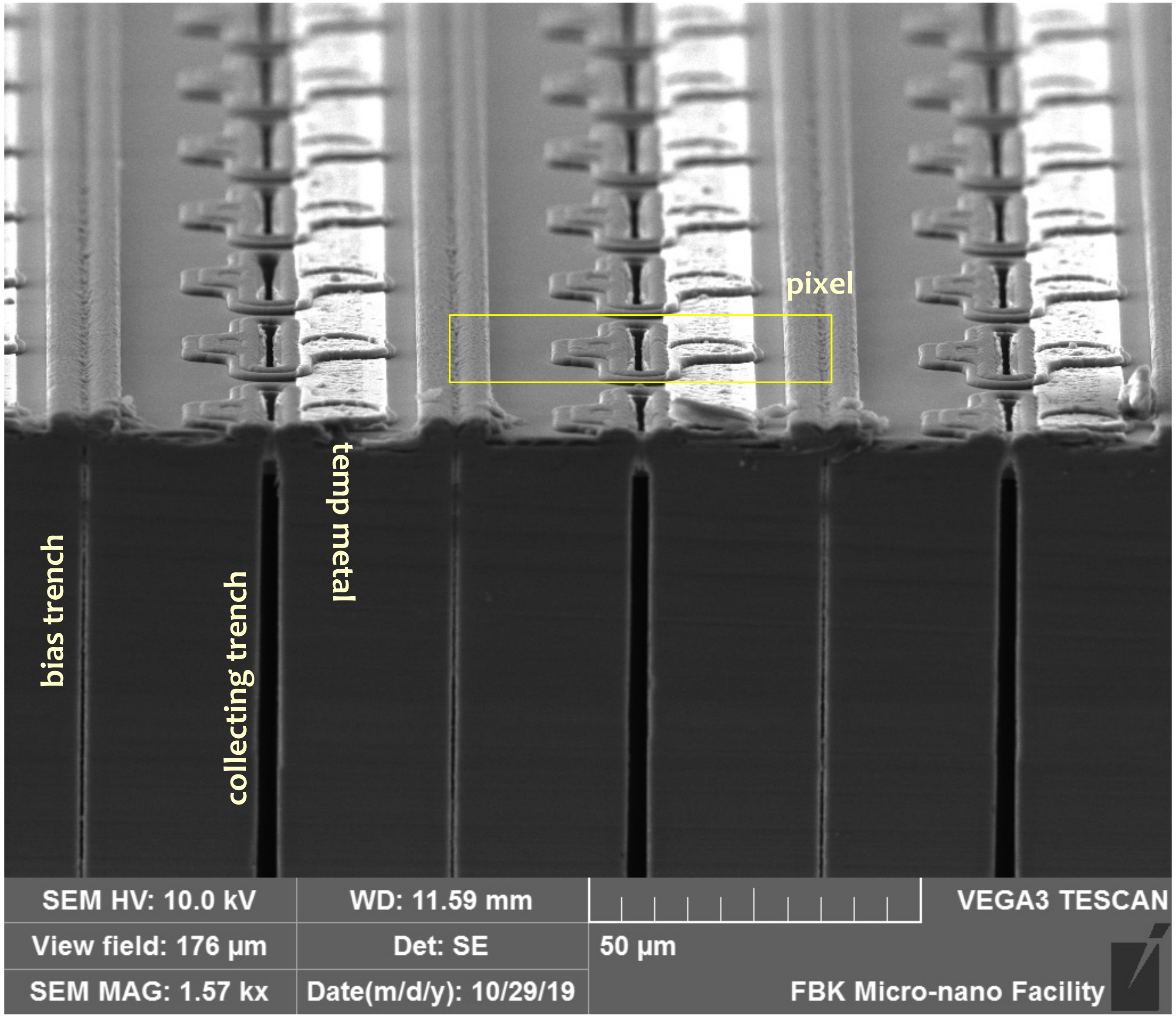

Deep Reactive Ion Etching
Bosch technology
(developed for MicroElectroMechanicalSystem technology)

First results on 3D-trench pixels at PSI (2019)

Time resolution of 3D-trench silicon pixels with MIPs (test-beam & lab) at room temperature

(ref. *Intrinsic time resolution of 3D-trench silicon pixels for charged particle detection*, 2020 JINST 15 P09029)

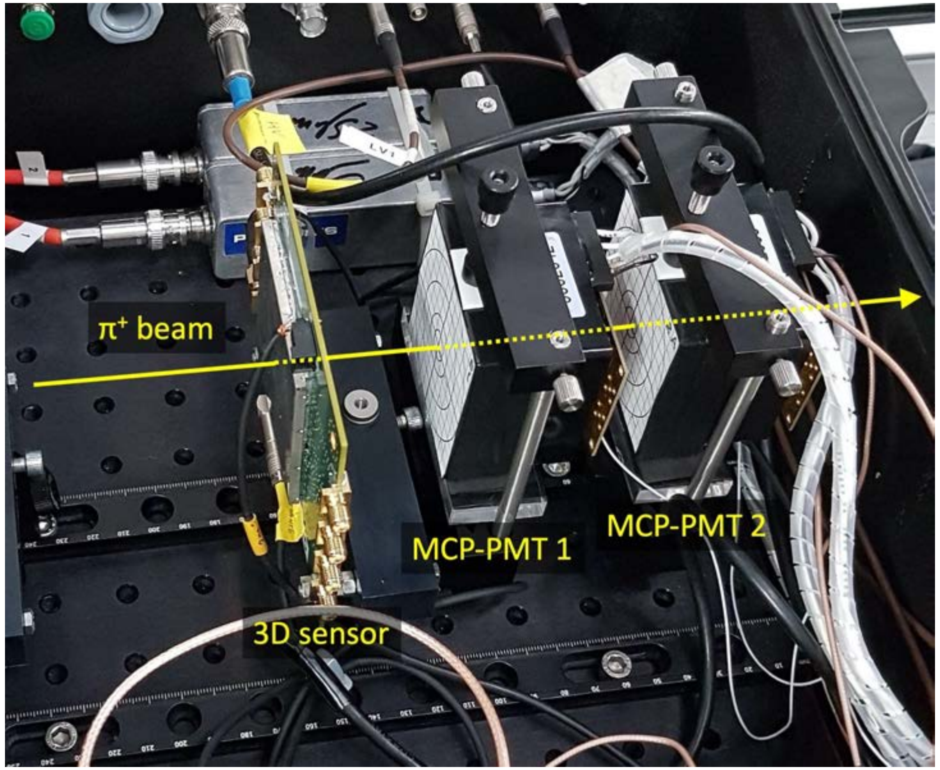

PSI πM1, π^+ beam, 270 MeV/c

Fast but not optimised FE used

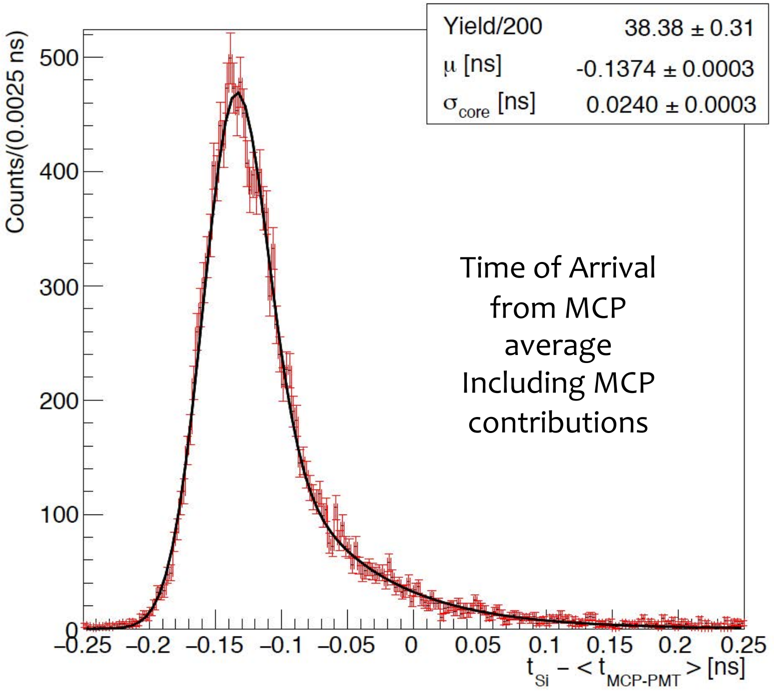

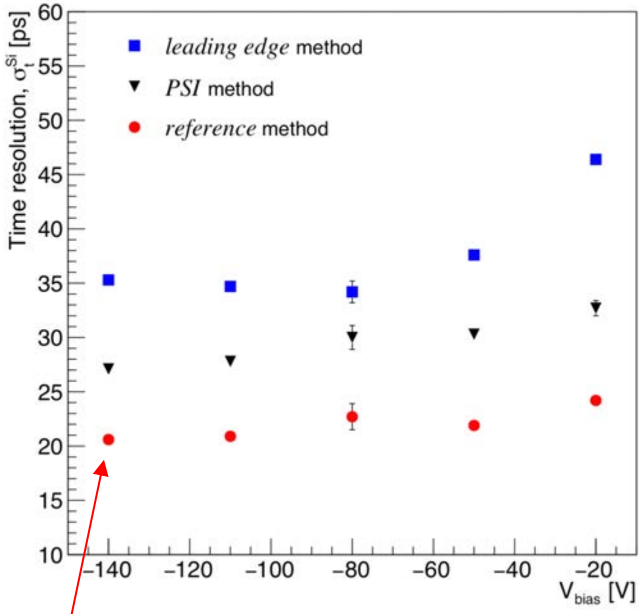

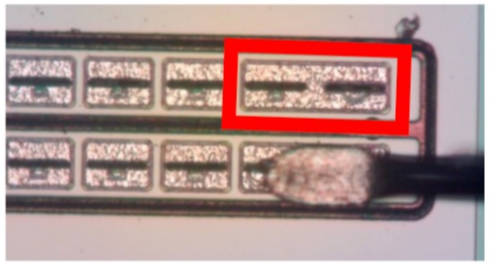

double pixel 55x110 μm²

$\sigma_t \approx 20$ ps

(after correction for MCP contribution) confirmed in corresponding laboratory measurements (with ^{90}Sr source)

An additional result from 2019 test beam

Separation of the electronics contribution and
first estimate of the "intrinsic" resolution of the sensor

$$\sigma_t = \sqrt{\sigma_{ej}^2 + \sigma_{un}^2}$$

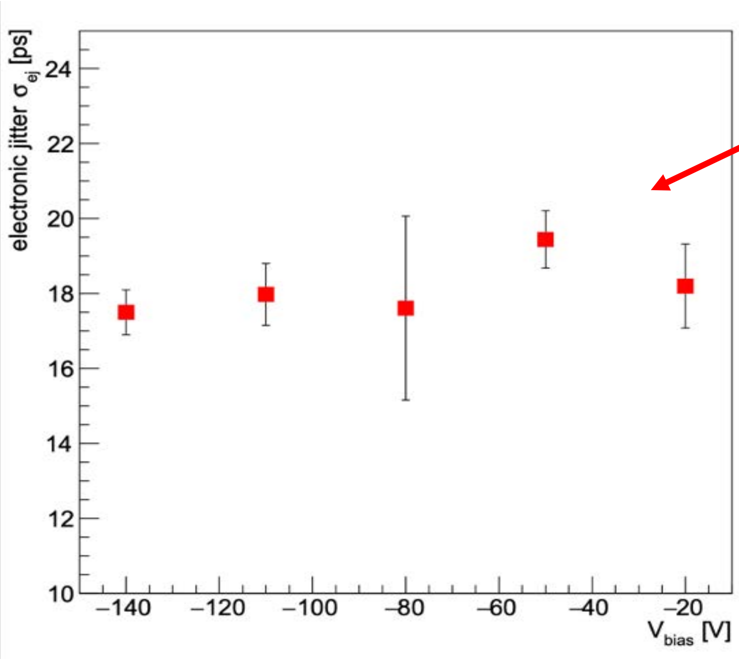

V_{bias} [V]	S/N	N [mV]	dV/dt [mV/ps]	σ_t^{Si} [ps]
−20	12.2	2.22	0.097	24.2 ± 0.5
−50	13.0	2.24	0.114	21.9 ± 0.4
−80	13.3	2.26	0.121	22.7 ± 1.2
−110	13.6	2.26	0.125	20.9 ± 0.4
−140	13.9	2.25	0.128	20.6 ± 0.4

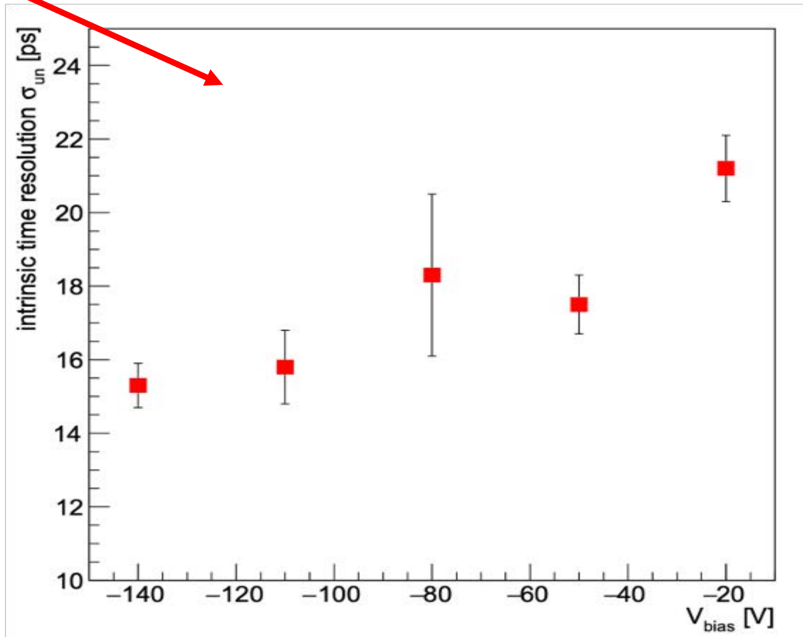

Intrinsic time resolution of a 3D-trench sensor σ_{un} (right) and contribution of the electronic jitter σ_{ej} (left) vs bias Voltage.

σ_t is obtainable as the quadrature sum of the two contributions.

σ_t is dominated by the contribution of the front-end electronics

L. Anderlini et al., *Intrinsic time resolution of 3D-trench silicon pixels for charged particle detection*, JINST 082 P0420 (2020); e-Print: arXiv:2004.10881v2.

A… tail story (of modeling)

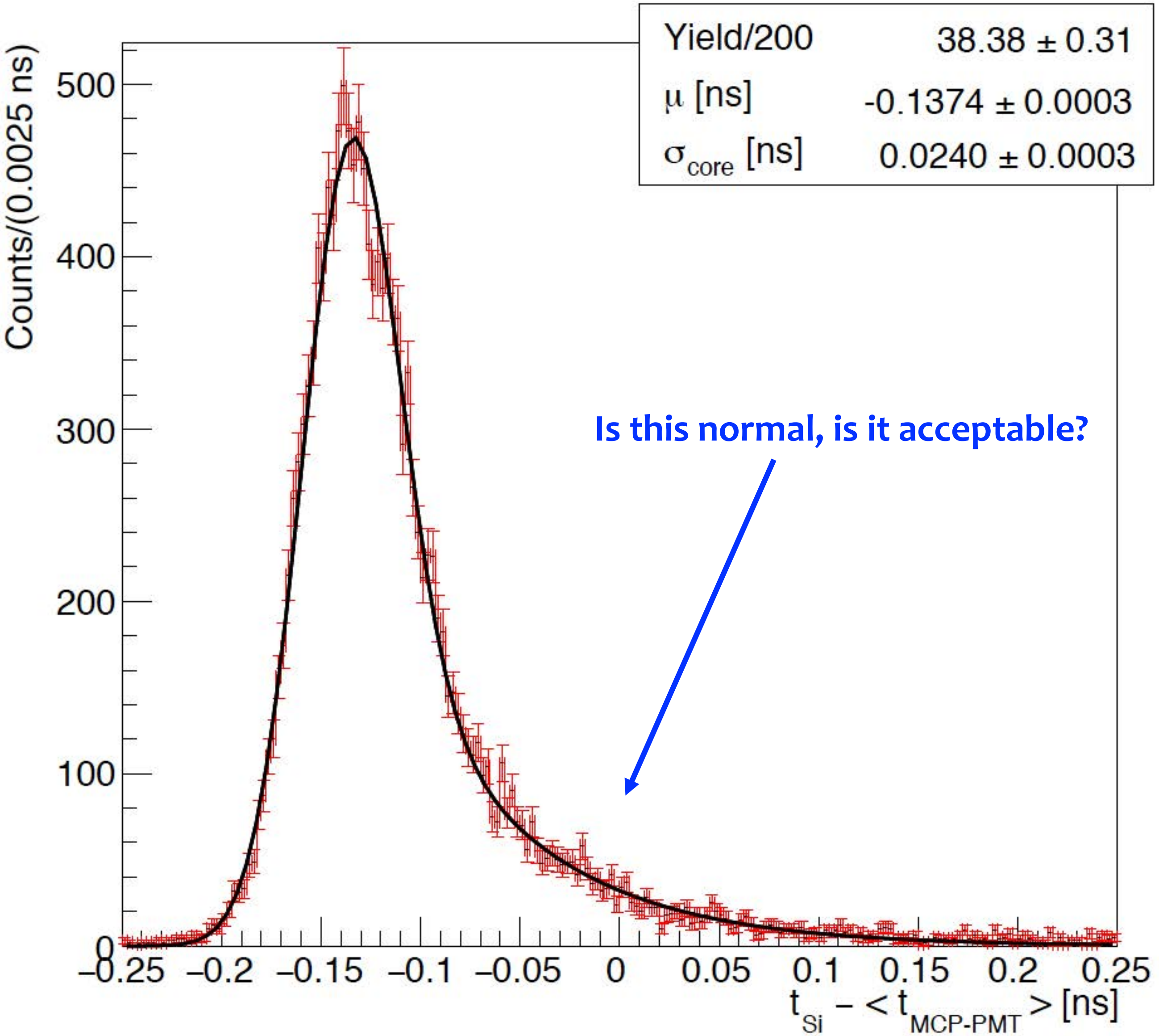

Is this normal, is it acceptable?

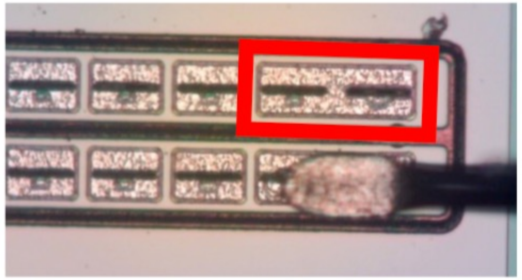

TCAD outputs

For detailed sensor charaterization

D. Brundu et al., *Accurate modelling of 3D-trench silicon sensor with enhanced timing performance and comparison with test beam measurements. JINST, 16, P09028*, 2021

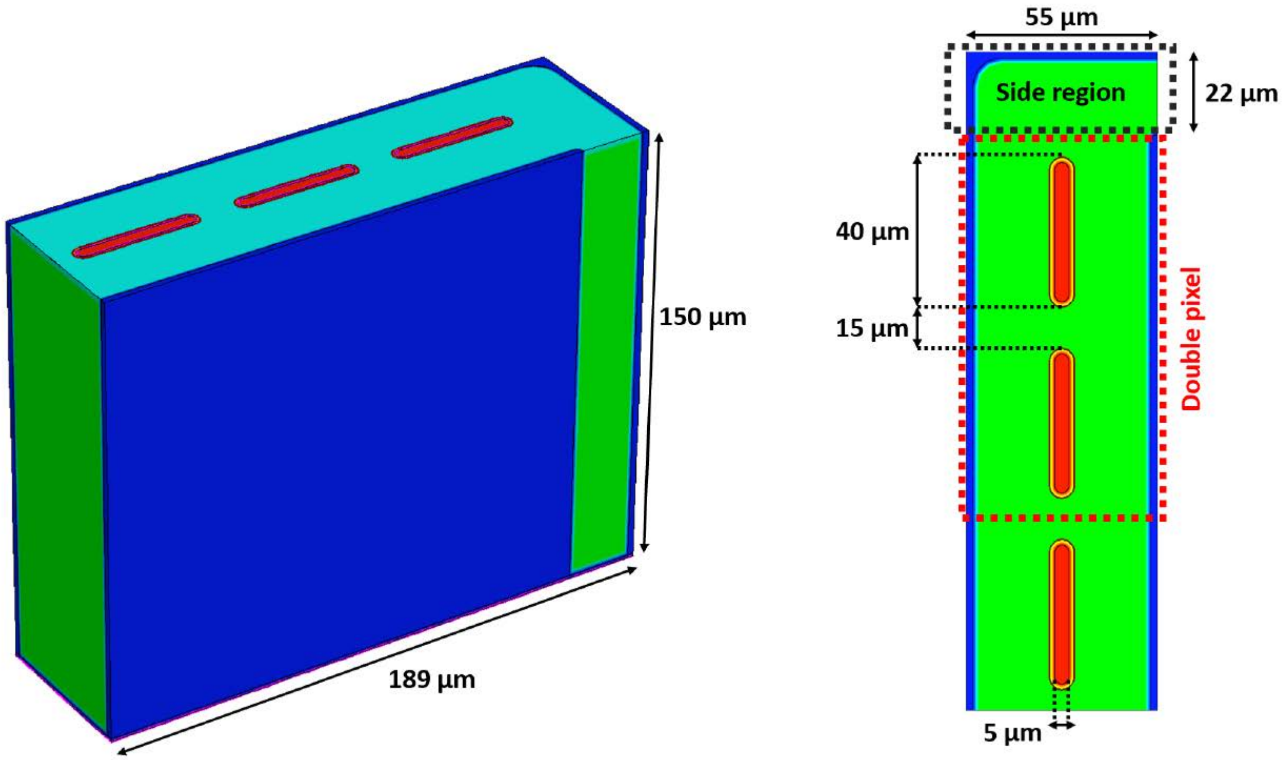

Layout of the simulated TimeSPOT test structure, including sections and sizes, designed using Sentaurus **TCAD**. The double pixel is indicated by the dotted-red line.

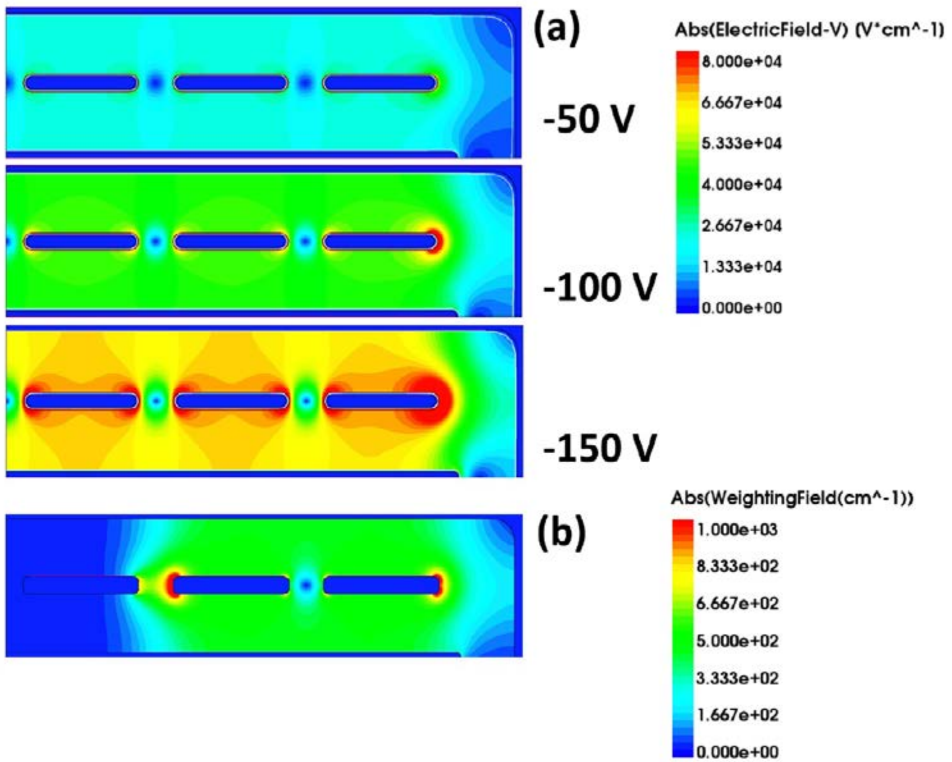

(a) Electric field amplitude at different bias voltages for the double-pixel test structure and
(b) weighting field

A virtual experiment on the DUT to identify tail contributions

Charge Collection Time distributions from TCoDe

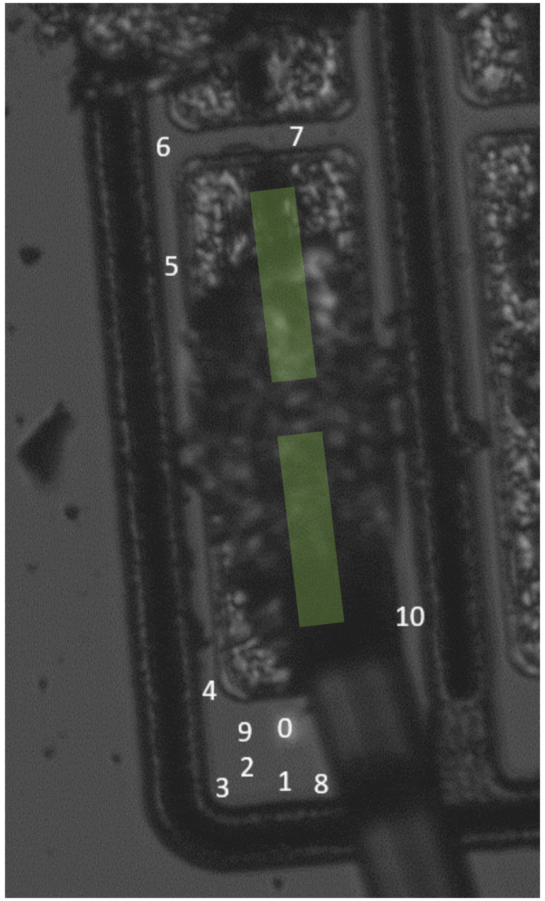

Double pixel structure under test @ PSI test-beam ($\sigma_t \approx$ 20 ps + exponential tail)

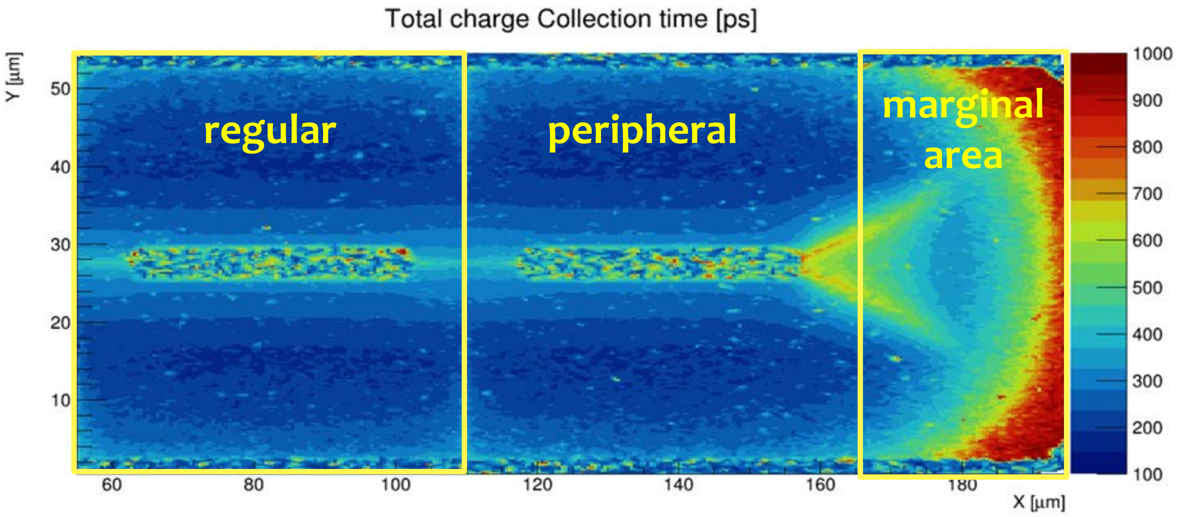

35k 270 MeV/c π^+ deposits **150 V bias**

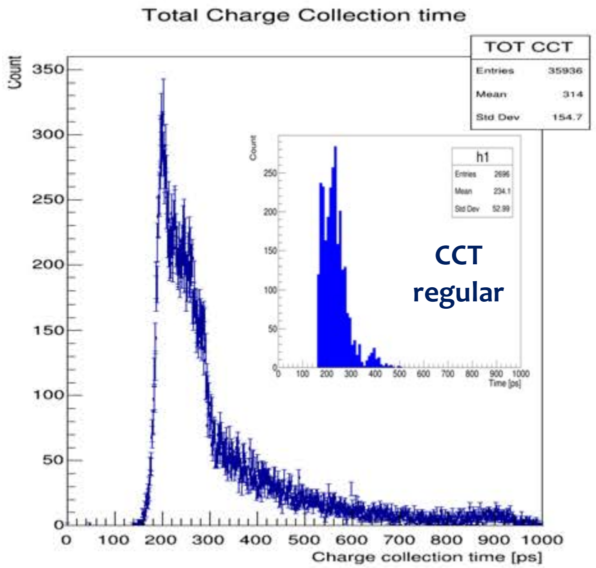

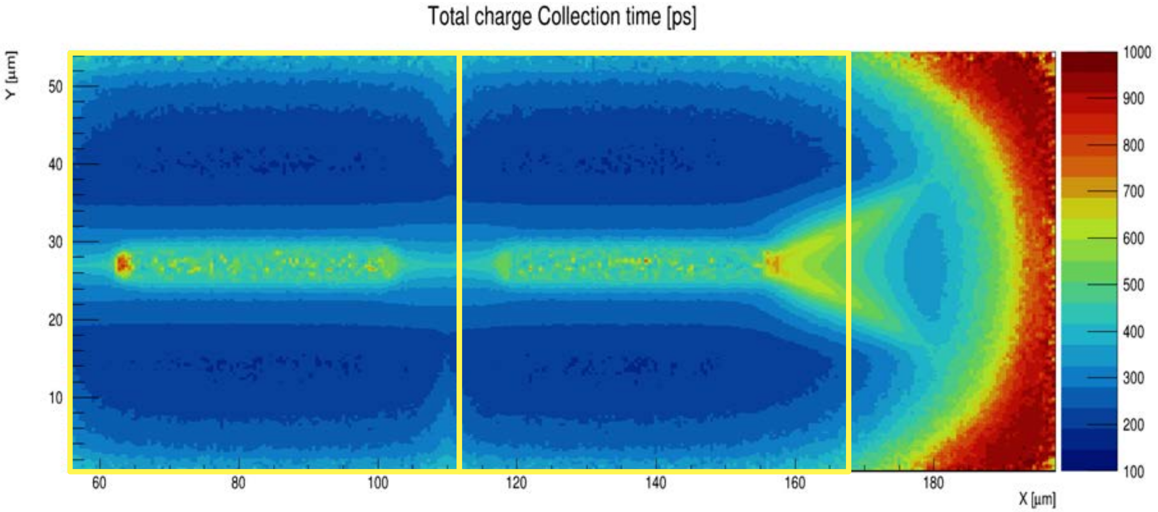

31k IR laser (MIP-like) deposits

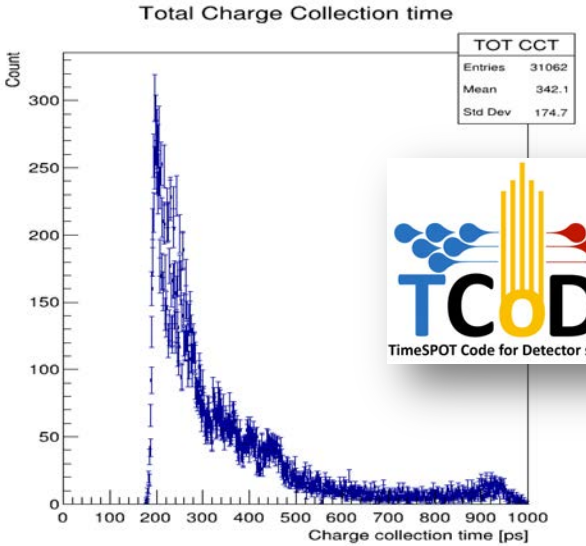

Before convolution

A. Loi – INFN Cagliari

F/E response? TFBoost!

TFBoost
TimeSPOT Front-end Booster

Brundu D, et al. (2022) Modeling of Solid State Detectors Using Advanced Multi-Threading: The TCoDe and TFBoost Simulation Packages. Front. Phys. 10:804752.

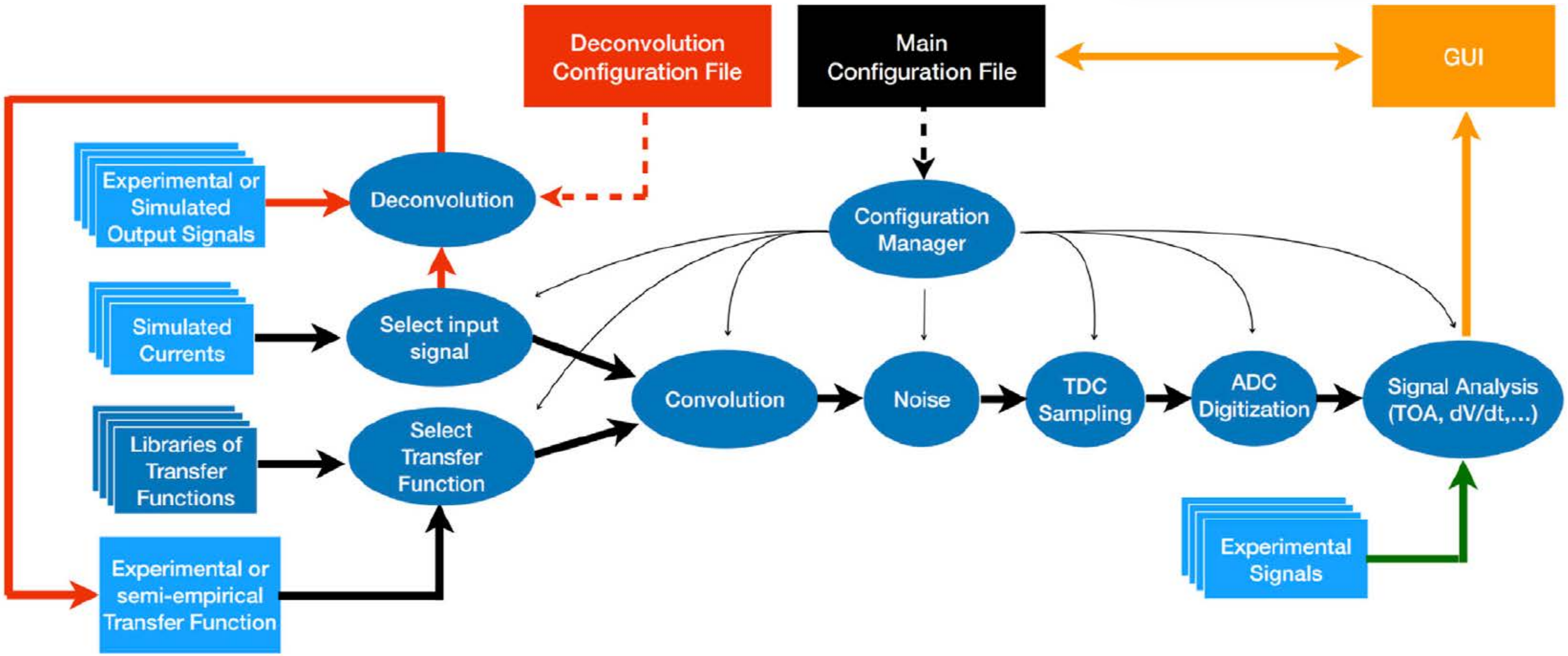

TFBoost simulations flow. The black path is the main simulation in which the convolution and the signal analysis are performed. The green path is followed if TFBoost is used as a pure signal analyzer, while the red path is followed to perform the deconvolution between an input current and an output signal.

TFBoost: TimeSPOT F/E model
emulation of experimental signals

TFBoost
TimeSPOT Front-end Booster

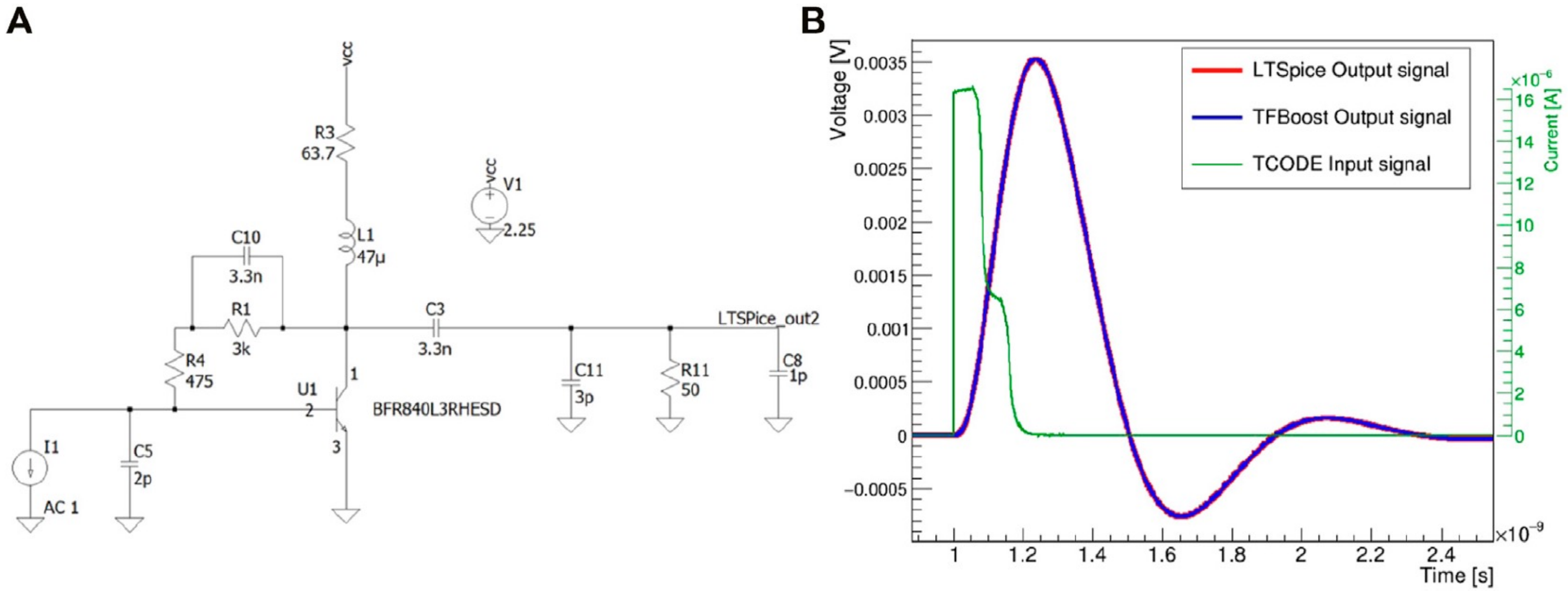

Spice simulation of a circuit that uses the spice model of a real SiGe bipolar transistor
(A) Comparison of the voltage output obtained using the same TCoDe input current in LTSpice and with TFBoost (B).

Brundu D, et al. (2022) Modeling of Solid State Detectors Using Advanced Multi-Threading: The TCoDe and TFBoost Simulation Packages. Front. Phys. 10:804752.

Full simulation chain outputs

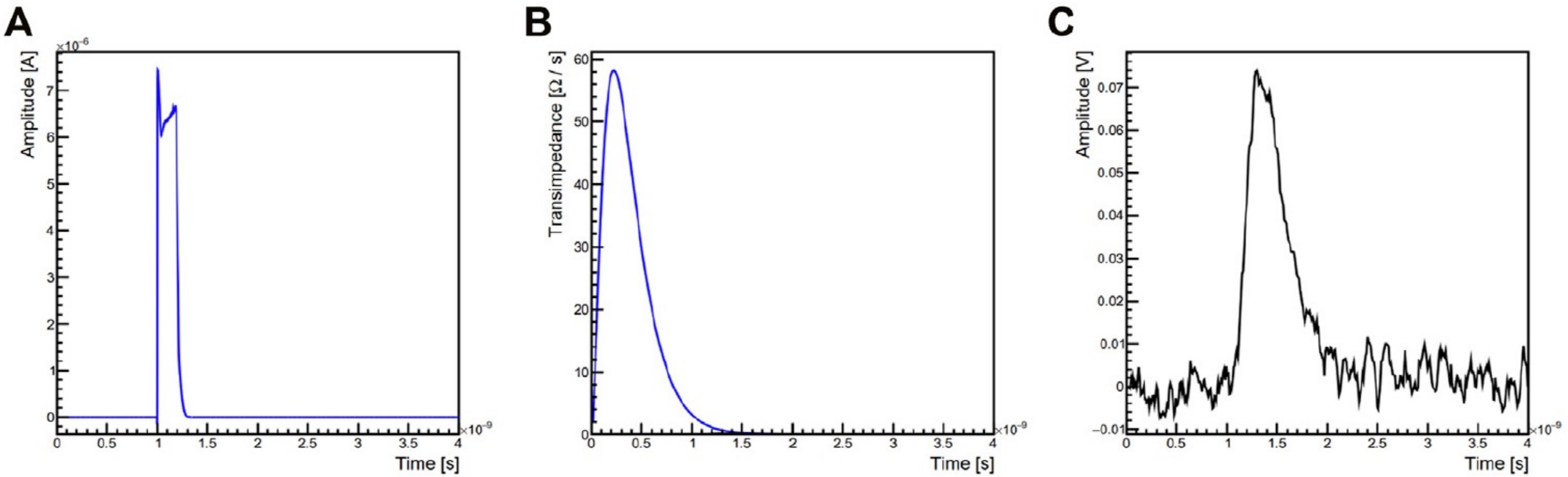

Example of the result of the front-end simulation for a single input current from TCoDe, for a 3D-trench double pixel structure at –150 V bias voltage:
(A) Input current for a MIP deposition in the sensor,
(B) simulated analytical transimpedance and
(C) output signal waveform with red noise (see next slides)

Brundu D, et al. (2022) Modeling of Solid State Detectors Using Advanced Multi-Threading: The TCoDe and TFBoost Simulation Packages. Front. Phys. 10:804752.

Transfer Function(s)

Analytical vs Semiempirical

out in TF

$$g(t) = f(t) \otimes h(t) = \int_{-\infty}^{+\infty} f(t)h(t-\tau)d\tau$$

convolution

t-domain

$$G(s) = F(s) \bullet H(s)$$

s-domain (Laplace transforms)

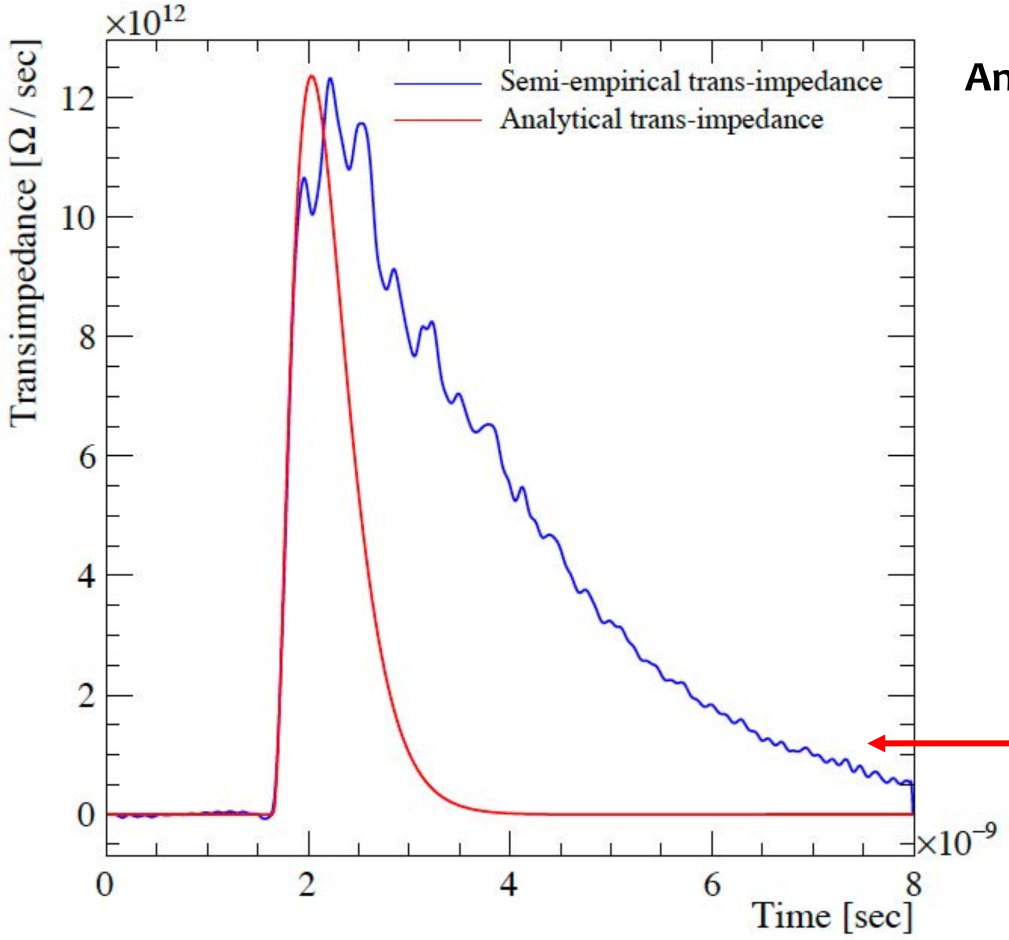

Analytical TF (from circuit generalized impedances in the s-domain)

$$\mathcal{R}(t) = \mathcal{L}^{-1}(t)\left\{-\frac{R_{m0}}{(1+s\tau)^2}\frac{G_0}{1+s\tau^*}\right\},$$

$$\mathcal{R}(t) = -G_0 R_{m0}\left\{\frac{(t(\tau-\tau^*)-\tau\tau^*)}{\tau(\tau-\tau^*)^2}e^{-\frac{t}{\tau}} - \frac{\tau^*}{(\tau-\tau^*)^2}e^{-\frac{t}{\tau^*}}\right\}.$$

The analytical transfer function, calculated from the circuit schematic (plus tentative corrections) is unable to take into account the complete set of contributions of the system (e.g. wire-bonding, long cables to scope, etc.)

Comparison between the analytical and semiempirical transfer functions (obtained by de-convolution)

Brundu D, et al. Accurate Modelling of 3d-Trench Silicon Sensor with Enhanced Timing Performance and Comparison with Test Beam Measurements. J Inst (2021)16:P09028.

Full simulation chain outputs

Semi-empirical approach

Brundu D, et al. Accurate Modelling of 3d-Trench Silicon Sensor with Enhanced Timing Performance and Comparison with Test Beam Measurements. J Inst (2021)16:P09028.

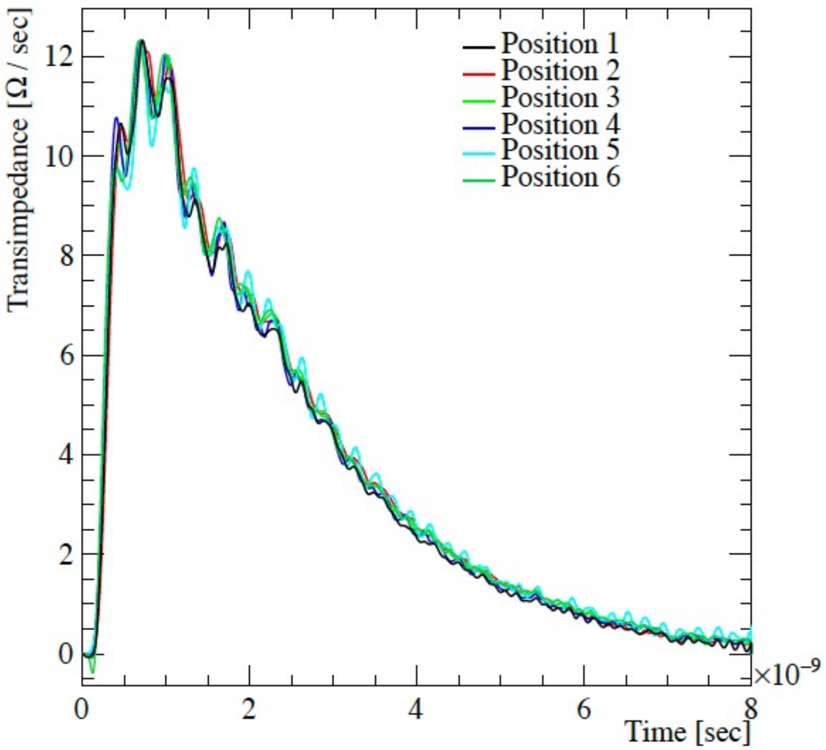

Comparison of semiempirical transfer functions obtained in different irradiation positions with the laser setup, for the –150V bias sample.

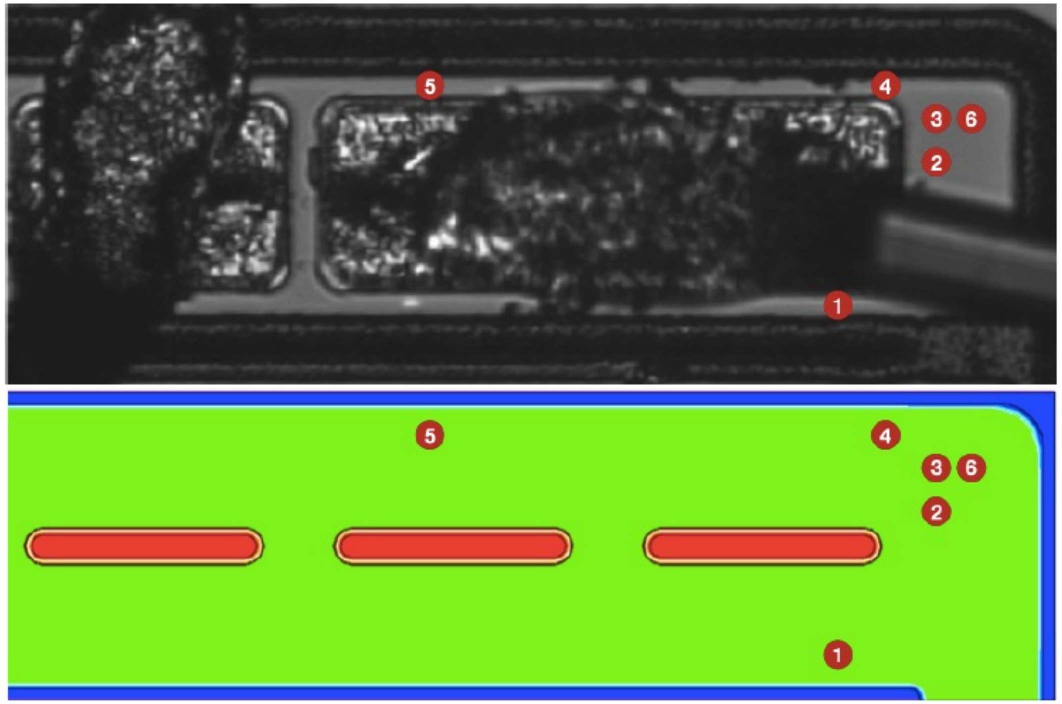

Six irradiation positions within the active area of the actual double-pixel test structure (top) and the corresponding positions in the simulated structure (bottom).
The current signals obtained from simulations were used to de-convolve the measured waveforms

$$g(t) = f(t) \otimes h(t) = \int_{-\infty}^{+\infty} f(t) h(t-\tau) d\tau$$

Use laser pulses to measure the $g(t)$ in well-known positions (output signal) → $f(t)$ is known (TCoDe signal current) → Deconvolve → $h(t)$ (semi-empirical TF)

Accurate re-analysis

Full simulation with noise contribution

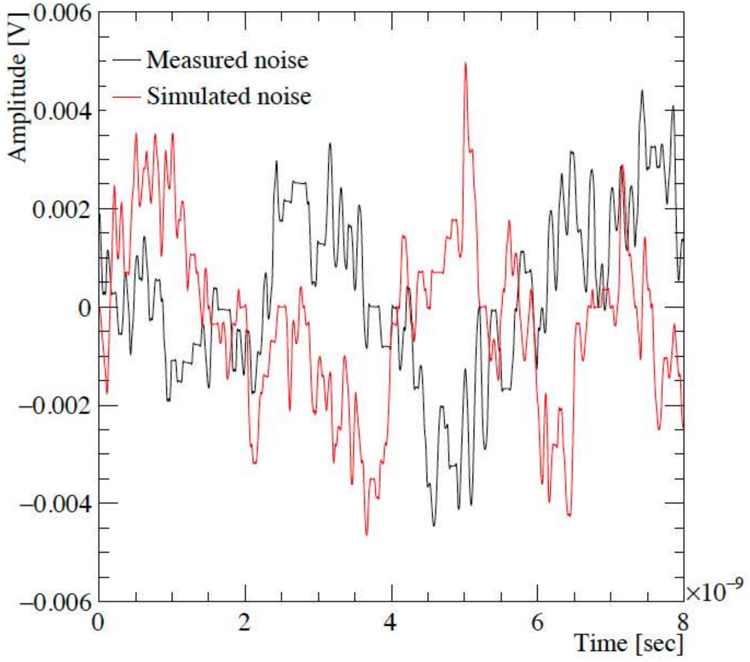

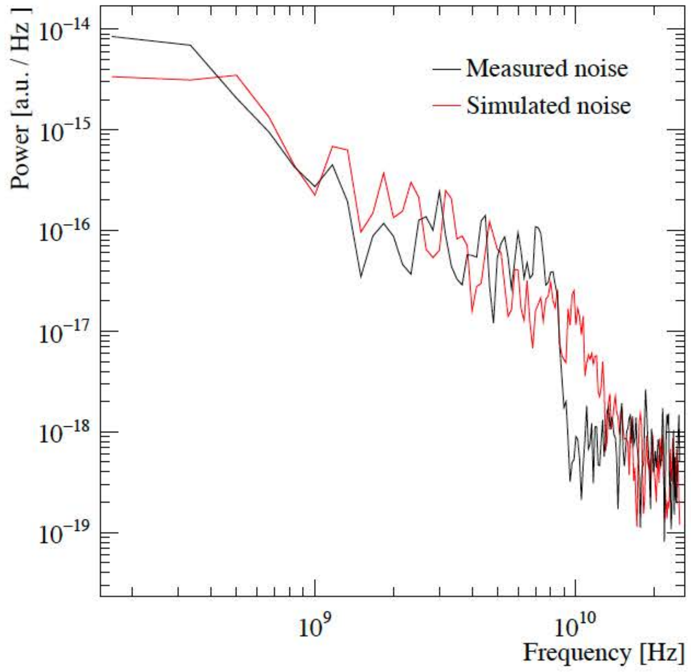

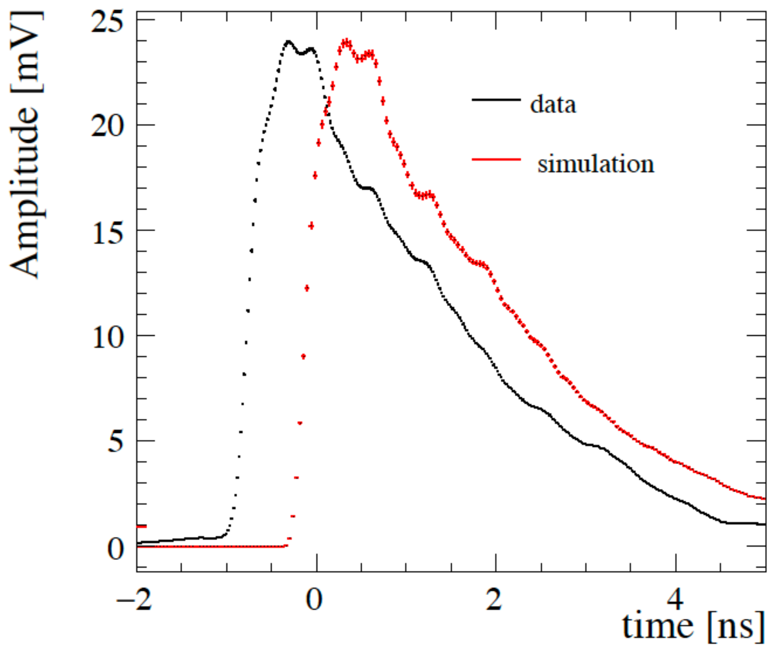

Comparison between two waveforms of (black) measured and (red) simulated noise for the –150V bias sample

Noise waveform in time domain: power spectral densities

Silicon sensor average waveform from the full (black) data and (red) simulation sample (about 30000 signals).
An arbitrary time shift between the two shapes is applied to allow a qualitative comparison

Brundu D, et al. Accurate Modelling of 3d-Trench Silicon Sensor with Enhanced Timing Performance and Comparison with Test Beam Measurements. J Inst (2021)16:P09028.

Accurate re-analysis

And the origin of the tails: simulation outputs

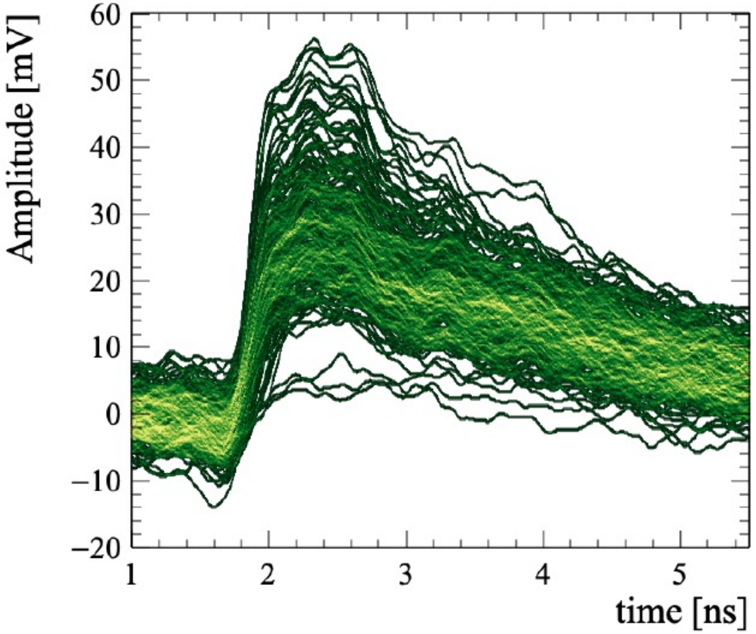

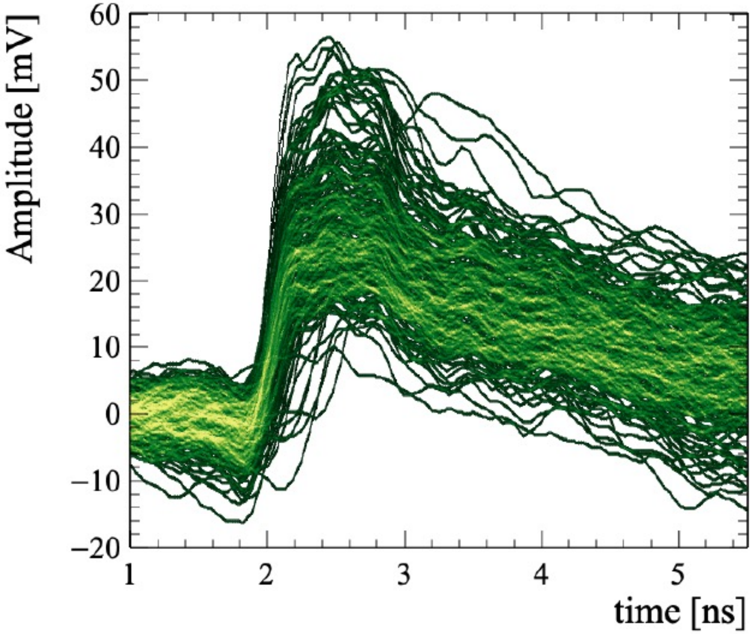

Overlap of all silicon sensor waveforms (about 200) for (left) simulation and (right) test beam data

	V_{bias} [V]	Amp(P_{max}) [mV]	⟨S/N⟩	⟨N⟩ [mV]	rise time [ps]	dV/dt [mV/ns]
Simulation	−50	25.0	14.6	2.11	247	103
	−100	24.5	14.3	2.17	224	113
	−150	24.4	14.2	2.19	217	116
Data	−50	24.1	14.3	2.19	258	111
	−110	24.4	13.9	2.30	221	123
	−140	24.7	14.2	2.29	217	126

Maximum amplitude, average signal-to-noise ratio, noise, rise time (20–80%) and slew rate (dV/dt) of the 3D-trench silicon sensor response at different values of the bias for simulation and data.
The statistical uncertainties are below 1%.

Brundu D, et al. Accurate Modelling of 3d-Trench Silicon Sensor with Enhanced Timing Performance and Comparison with Test Beam Measurements. J Inst (2021)16:P09028.

Final response about the slow tails

The very special case of the double pixel

D. Brundu et al., Accurate modelling of 3D-trench silicon sensor with enhanced timing performance and comparison with test beam measurements. *JINST, 16, P09028*, 2021

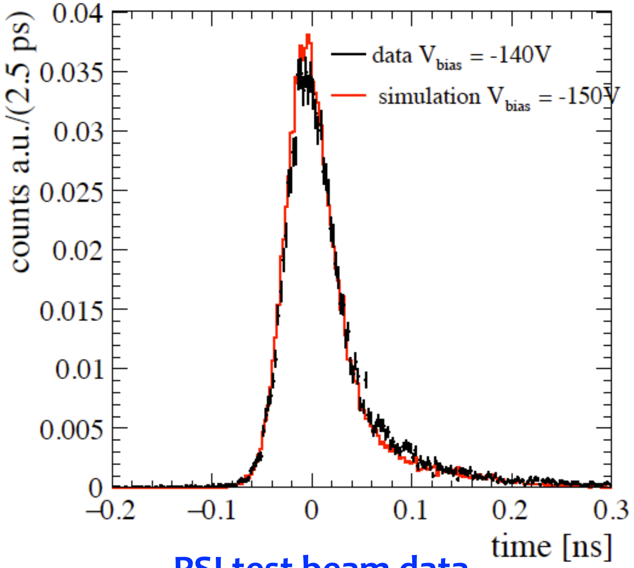

PSI test beam data

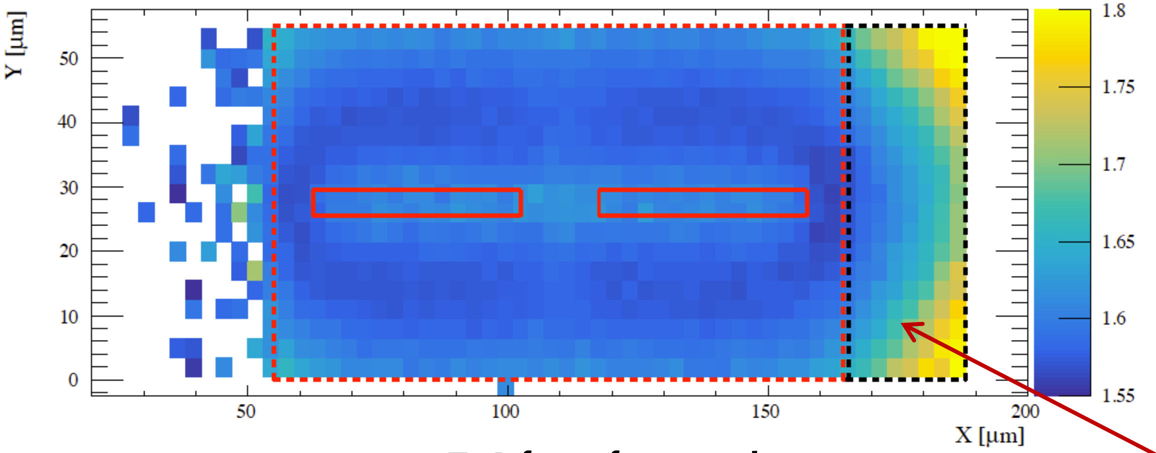

ToA from front-end

Simulated data

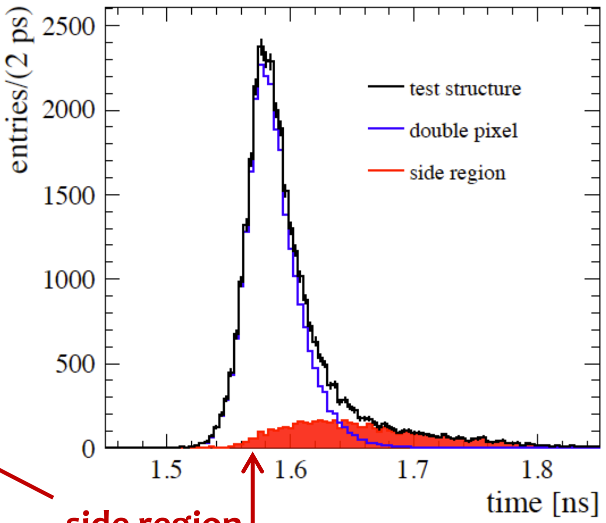

side region

Simulation			Measurement	
V_{bias} [V]	$\sigma_{intrinsic}$ [ps]	σ_t [ps]	V_{bias} [V]	σ_t [ps]
−50	9.6 ± 0.1	18.9 ± 0.2	−50	20.7 ± 0.3
−100	8.0 ± 0.1	16.7 ± 0.2	−110	19.8 ± 0.2
−150	7.0 ± 0.1	16.3 ± 0.2	−140	19.0 ± 0.2

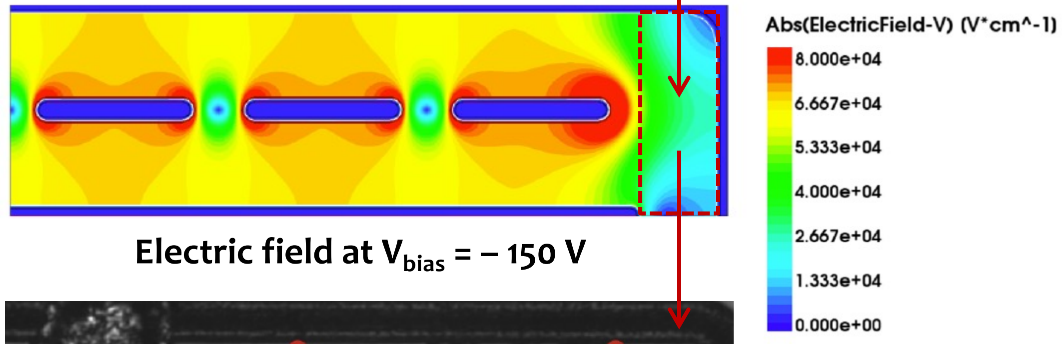

Electric field at V_{bias} = – 150 V

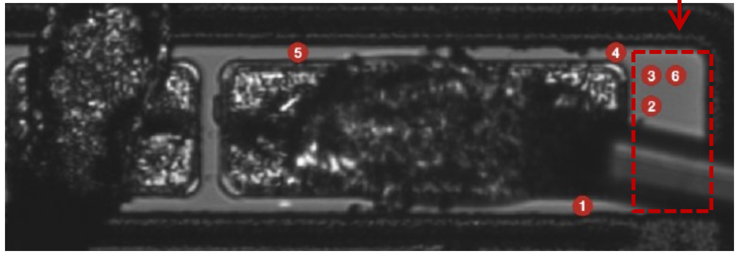

Double pixel picture

Tails have been studied with very accurate pixel modeling, from the ionization process to the front-end output.
A clear assignation of the tail contribution was done to the (out)side region of the pixel (outside the nominal pixel area in this particular case).
As a by-product, simulations clearly indicate a better intrinsic performance of the sensor

Tails, efficiency and time resolution

Experimental comparison with other geometries

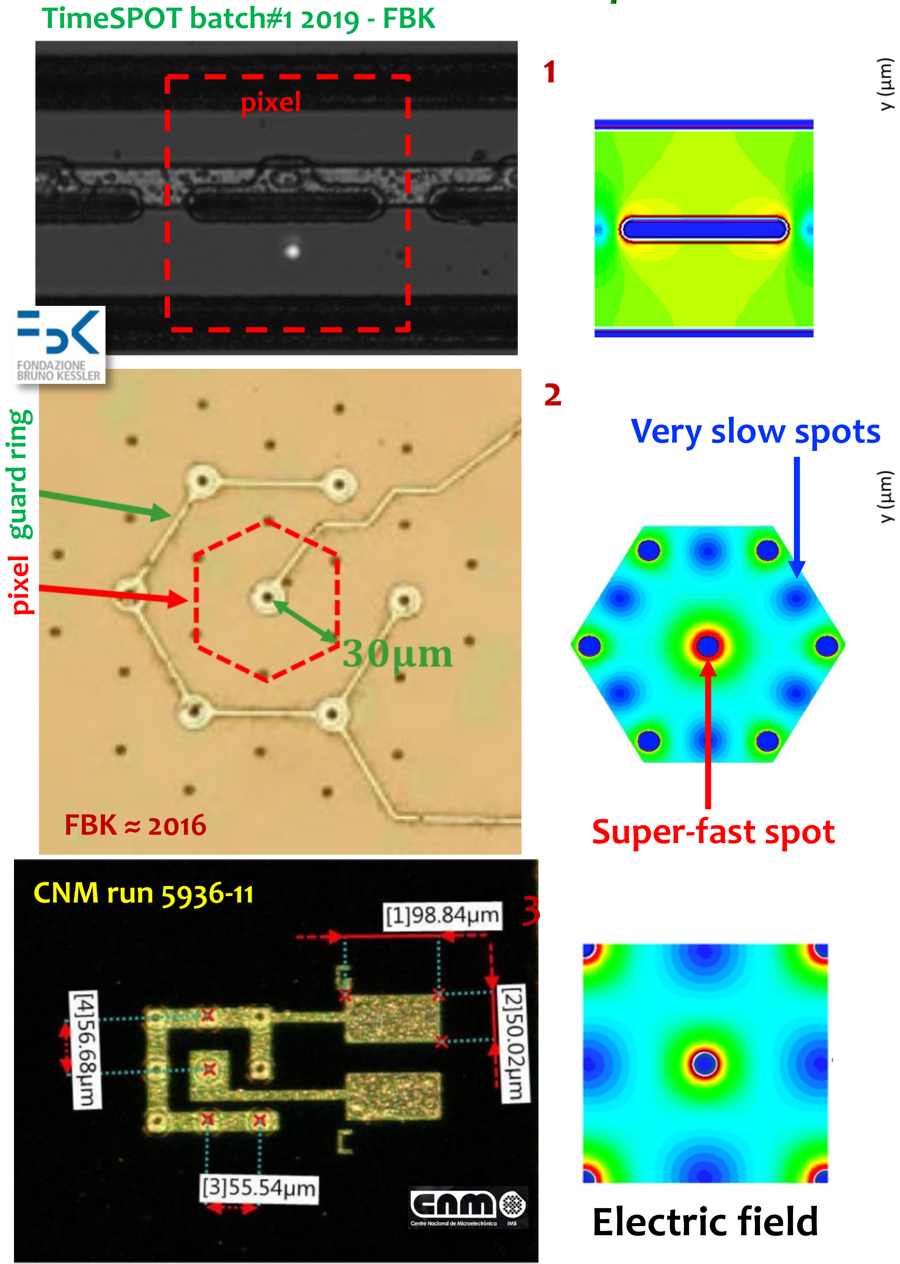

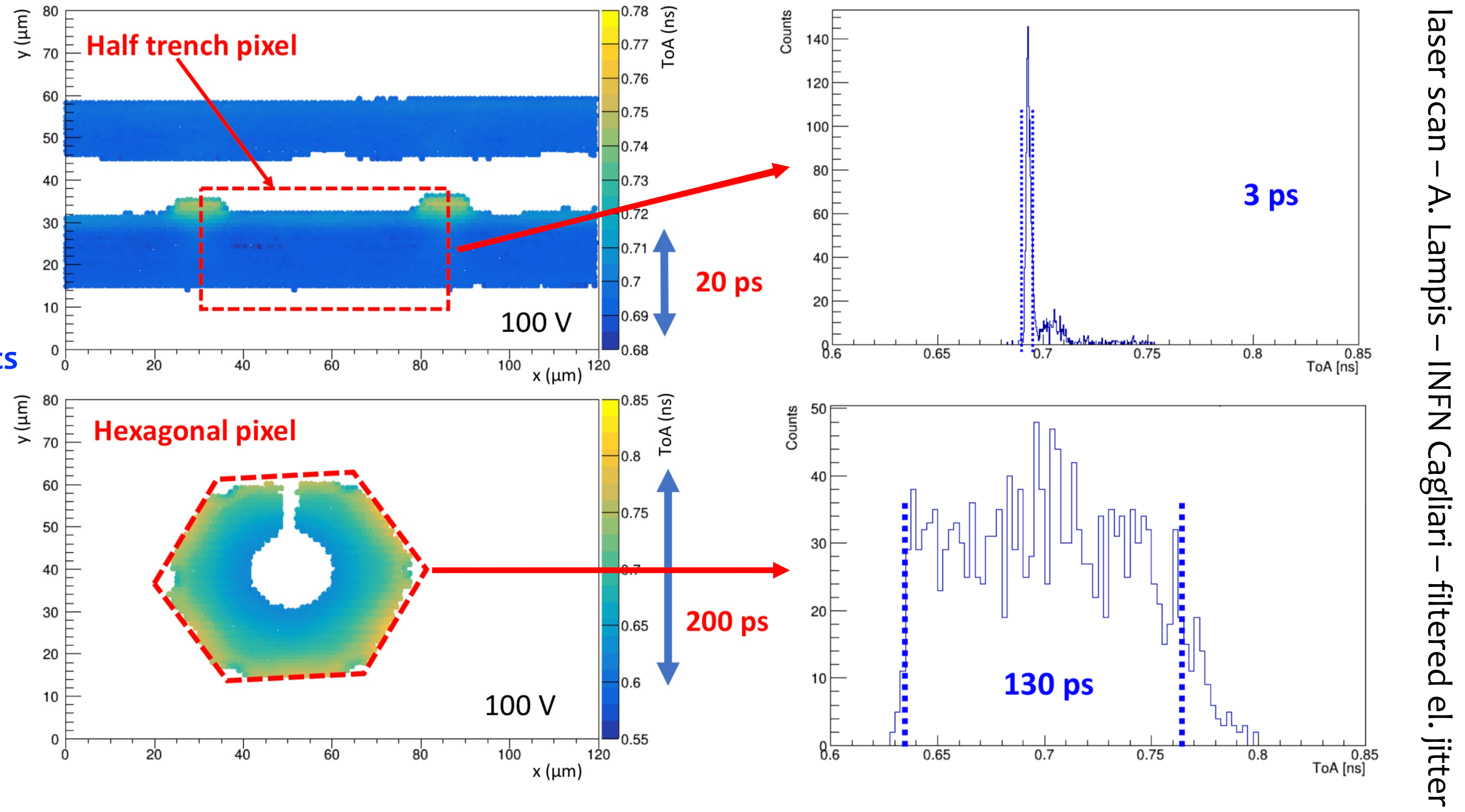

- In 3D sensors, the key for resolution is geometry (uniformity), not speed
- Extended slow spots give tails which cannot be cut-off arbitrarily
- They can give also substantial inefficiency in detection
- It is important to cross-check resolution with efficiency in order to perform a correct (un-biased) resolution measurement

Tests on the geometric (in)efficiency

And more timing tests at SPS/H8 with new F/E electronics (Nov'21)

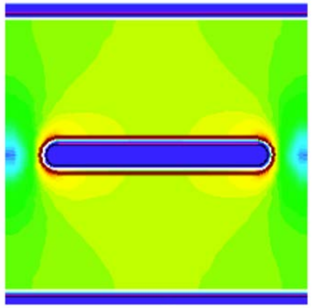

Blue areas are "dead" for orthogonal tracks
The sensor must be operated with a tilt angle.

New faster dedicated front-end electronics

Si-Ge input stages $t_r \approx 100$ ps.
Measured *jitter* < 7 ps @ 2 fC

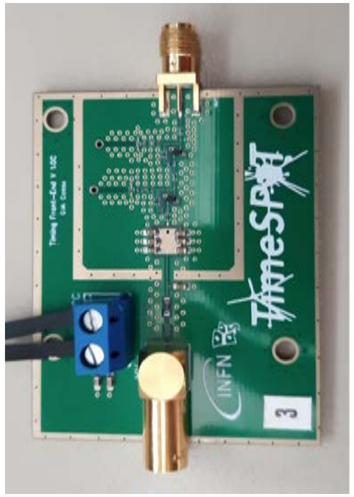

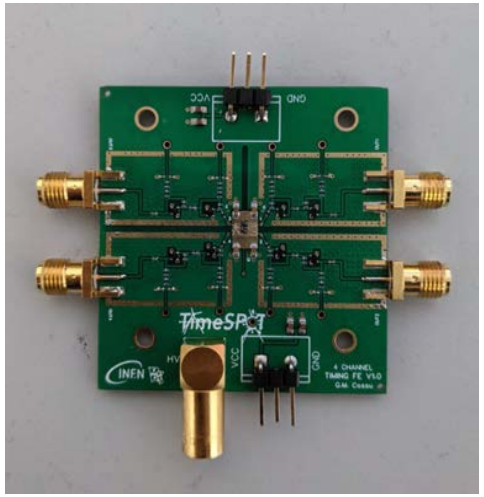

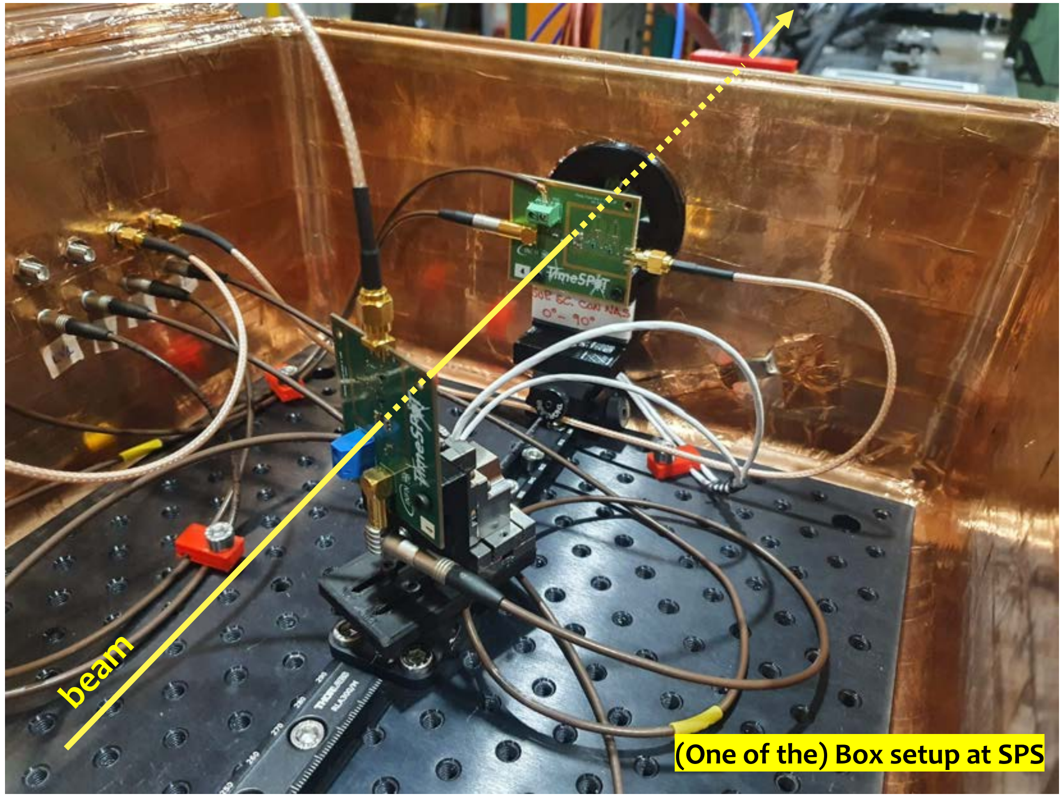

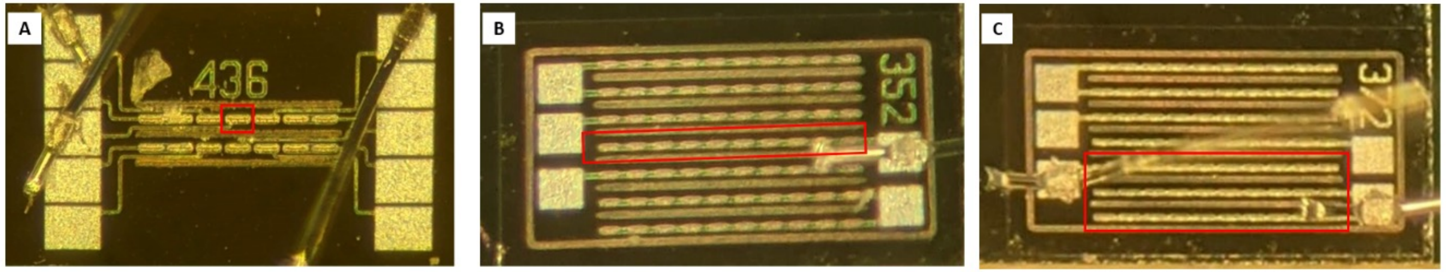

Tested structures. For each sensor the active area is shown in red. (A) Single pixels sensor; (B) strip sensor; (C) triple strip sensor

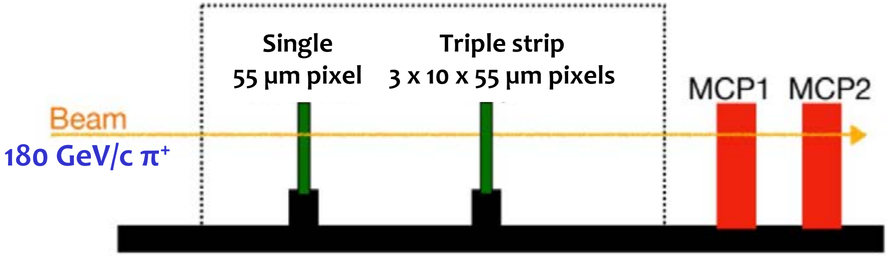

Improved setup

3D silicon sensors are mounted inside a shielded box. The two MCP-PMTs are placed downstream, outside the box. Three different types of board holder were used: the fixed mount holding the reference sensor, a mount with manual translation stages with micrometric accuracy and a mount with x-y piezoelectric motor linear stages with a 10 nm accuracy.

Paper in preparation:
***"New results on the TimeSPOT 3D-silicon sensors from measurements at SPS"* (Frontiers in Physics)**

New timing measurements

(pixel @ α_{tilt} = 0 °) SPS/H8 (Nov’21)

Paper to be submitted soon to Frontiers in Physics: *“New results on the TimeSPOT 3D-silicon sensors from measurements at SPS”*

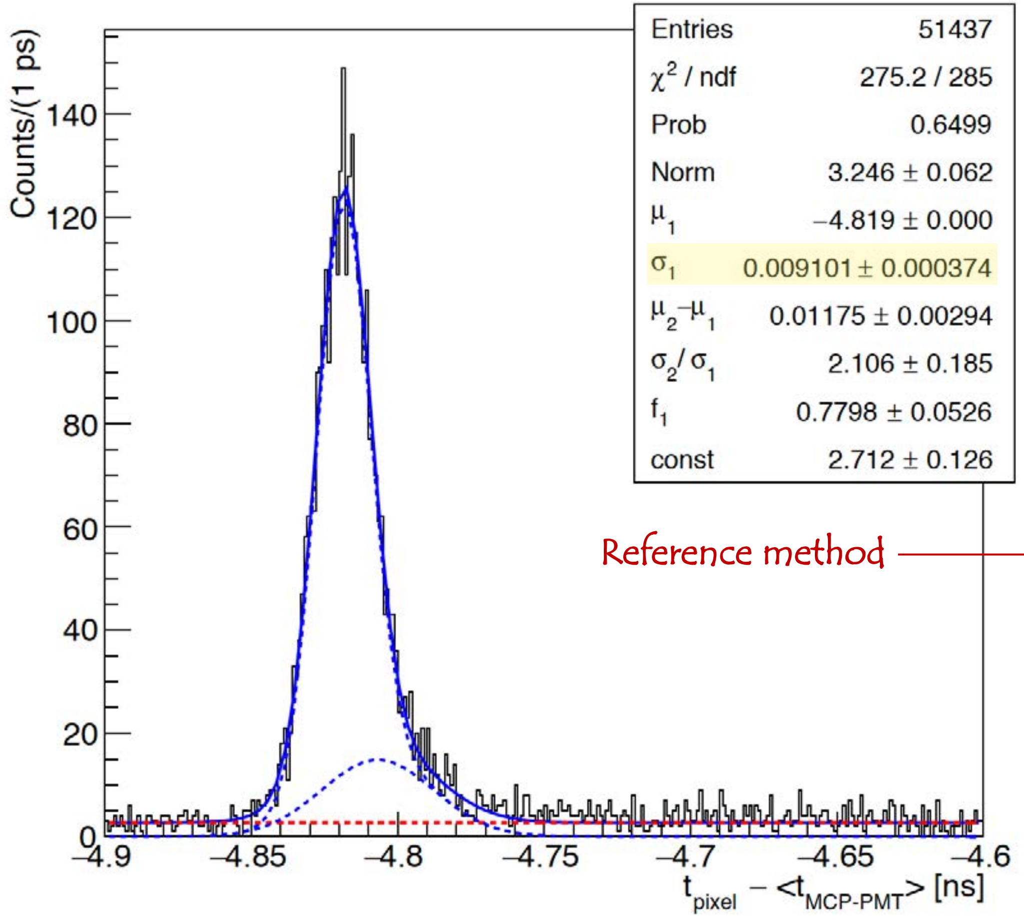

Distribution of the difference between the TOA of the single pixel and the time reference, $t_{pixel} - \langle t_{MCP-PMT} \rangle$, for the single pixel perpendicular to the beam at V_{bias} = −100 V with the reference method. The distribution is fit with the sum of two Gaussian functions (blue dashed lines) describing the signal, and a constant (red dashed line) modelling the background.

Reference method

σ_t^{eff} 11.5 ps

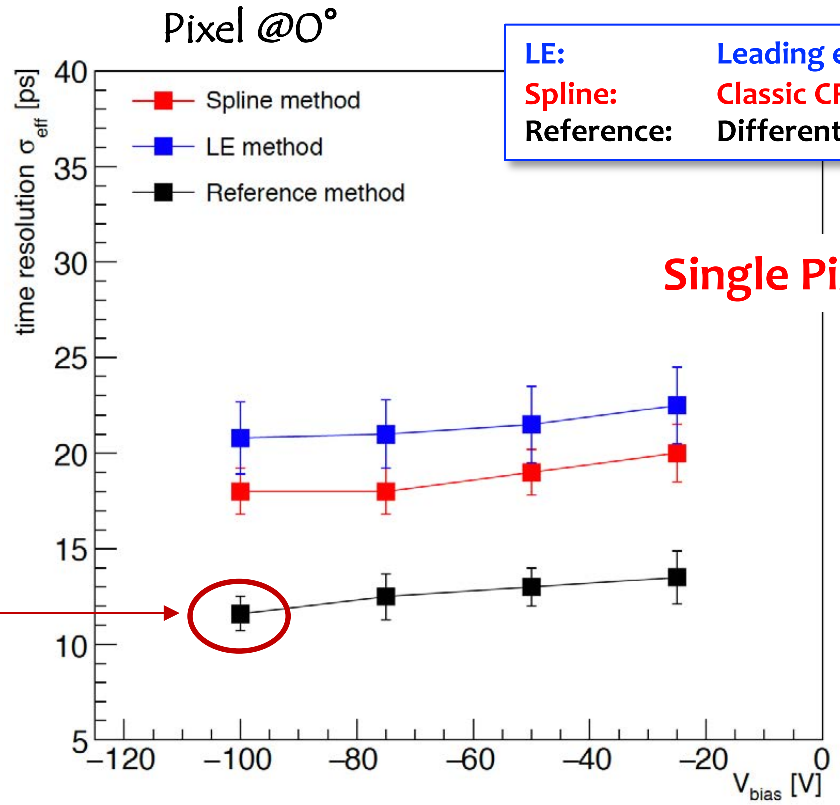

LE:	**Leading edge, no ToT correction**
Spline:	**Classic CFD**
Reference:	**Differentiation + CFD**

Single Pixel @ 100V

$$(\sigma_t^{\mathrm{eff}})^2 = f_1(\sigma_1^2 + \mu_1^2) + (1 - f_1) \cdot (\sigma_2^2 + \mu_2^2) - \mu^2$$

Where f_1 is the fraction of the core Gaussian and μ is defined as

$$\mu = f_1\mu_1 + (1 - f_1) \cdot \mu_2$$

σ_t^{eff} **takes into account the two-Gaussian behaviour**

Efficiency: results

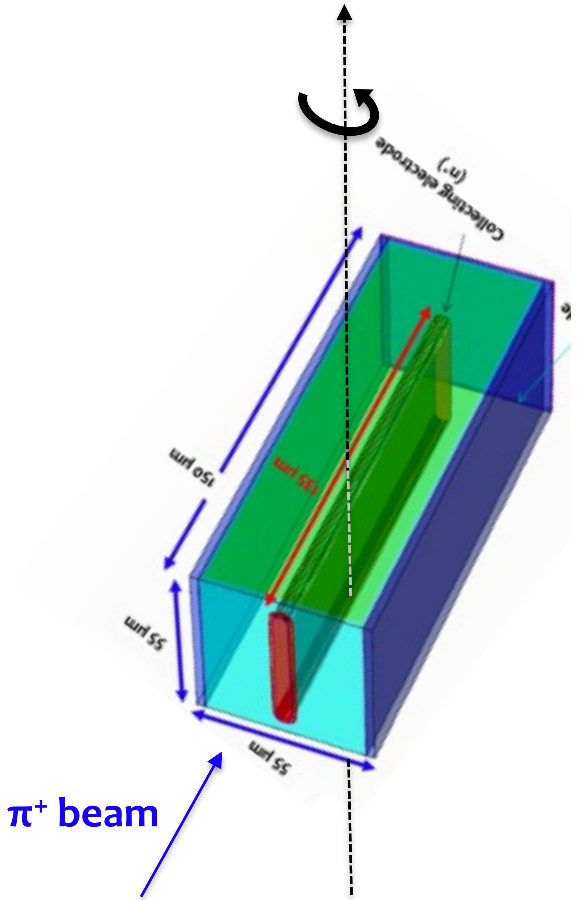

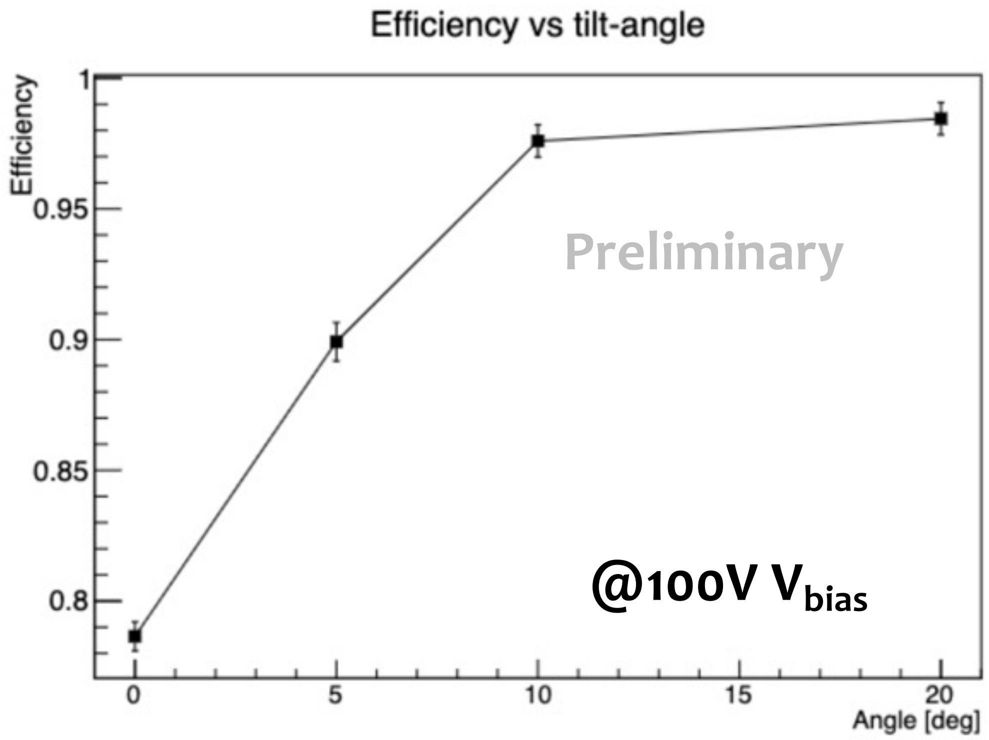

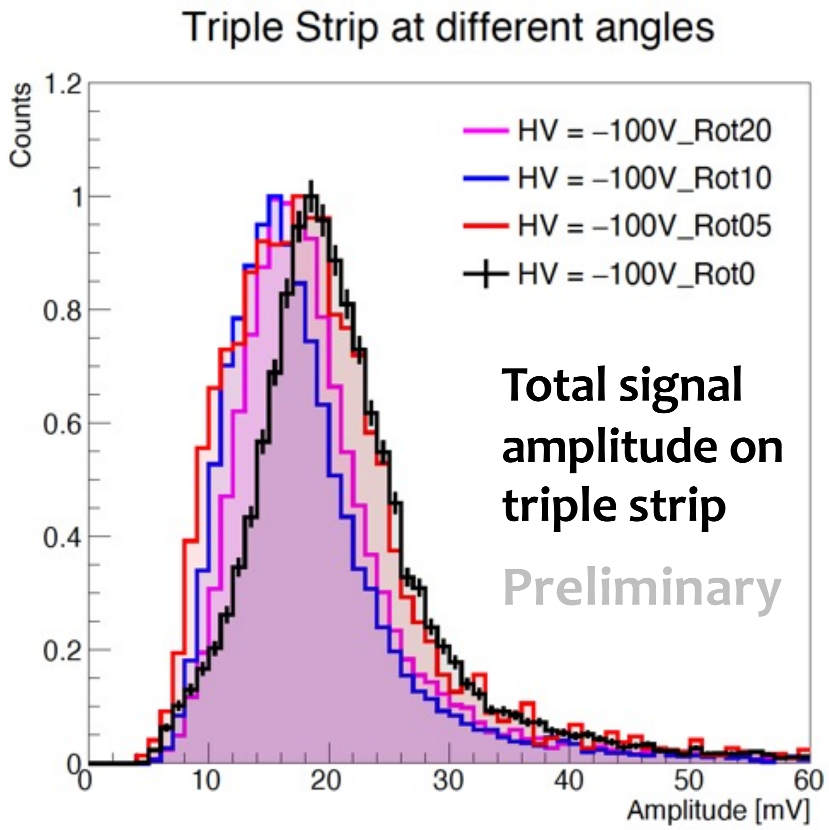

The inefficiency (at normal incidence) due to the 3D pixel dead-area of the trenches is fully recovered by tilting the sensors around the trench axis at angles larger than 10°

Tilted sensors: timing performances

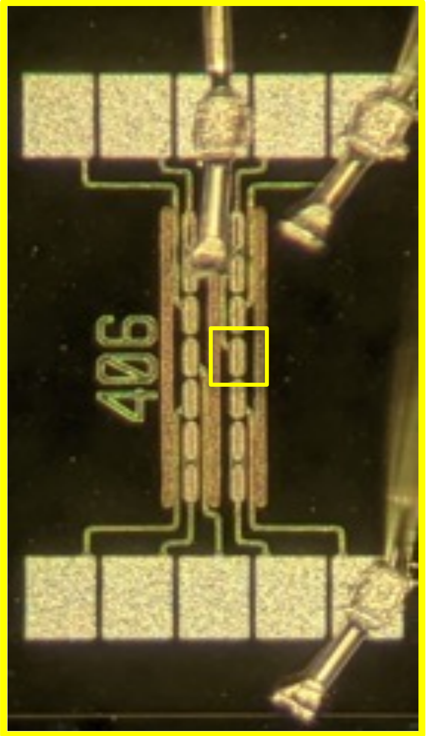

Does some tilt (rot. 1) slightly improves the time resolution?

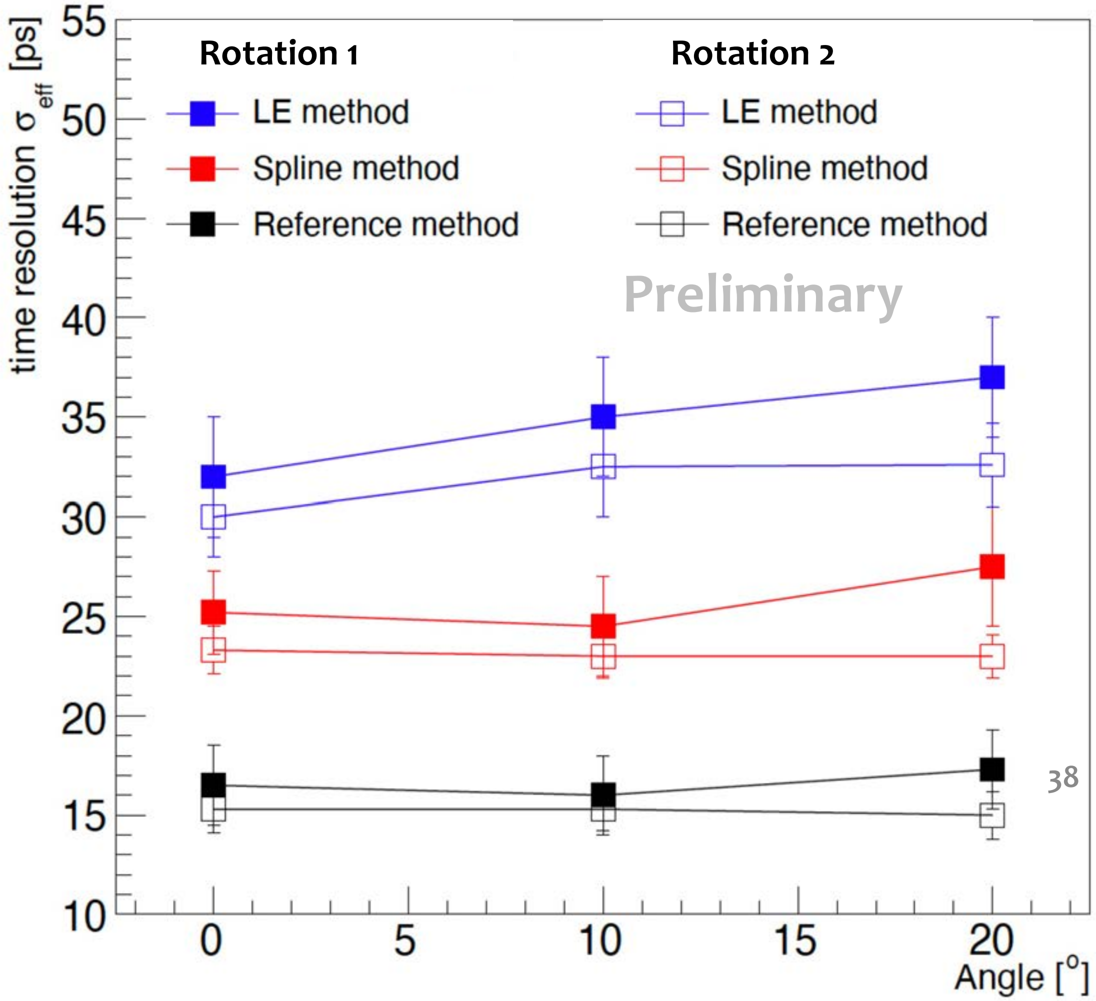

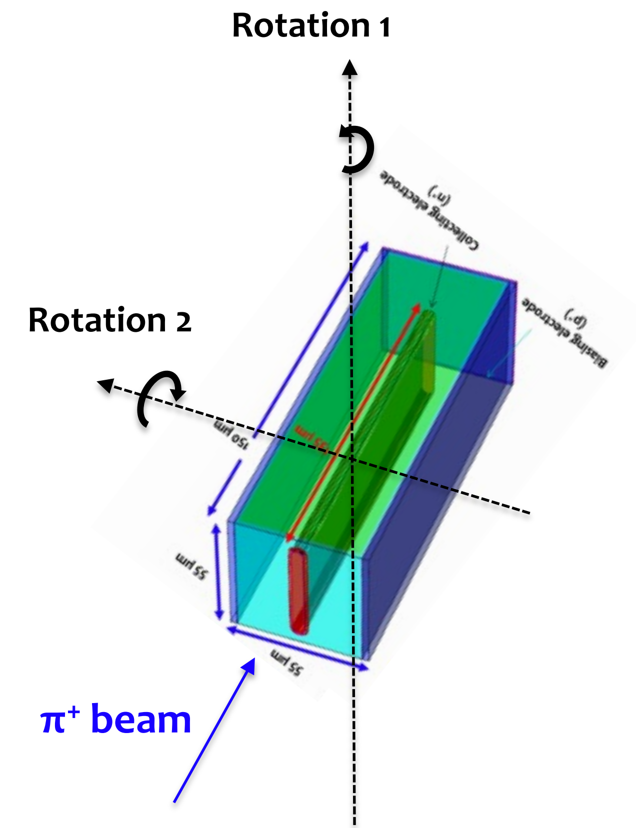

Single Pixel @ 50V

Effect of tilting on distribution shapes

Spline method, SPS/H8 (Nov'21)

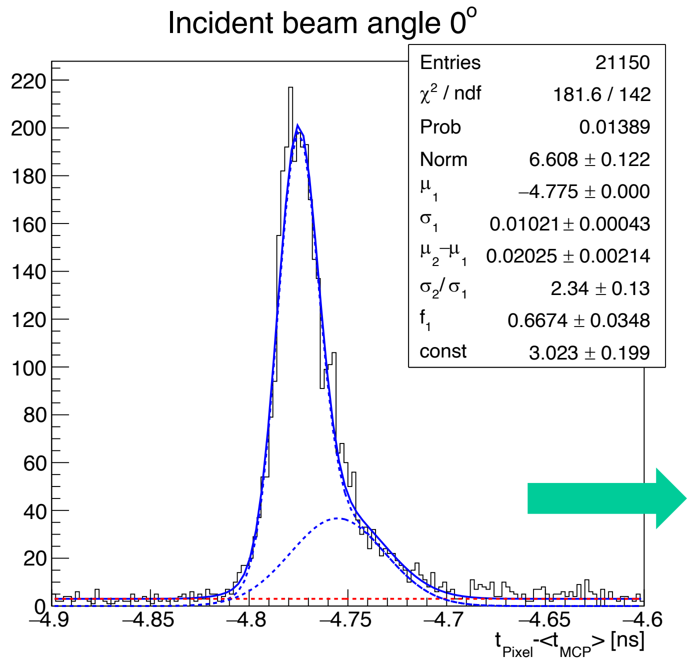

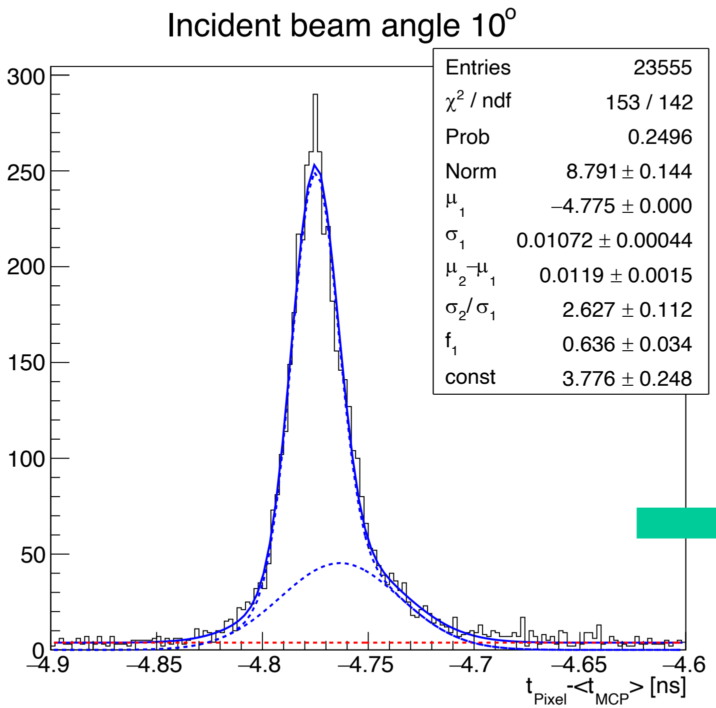

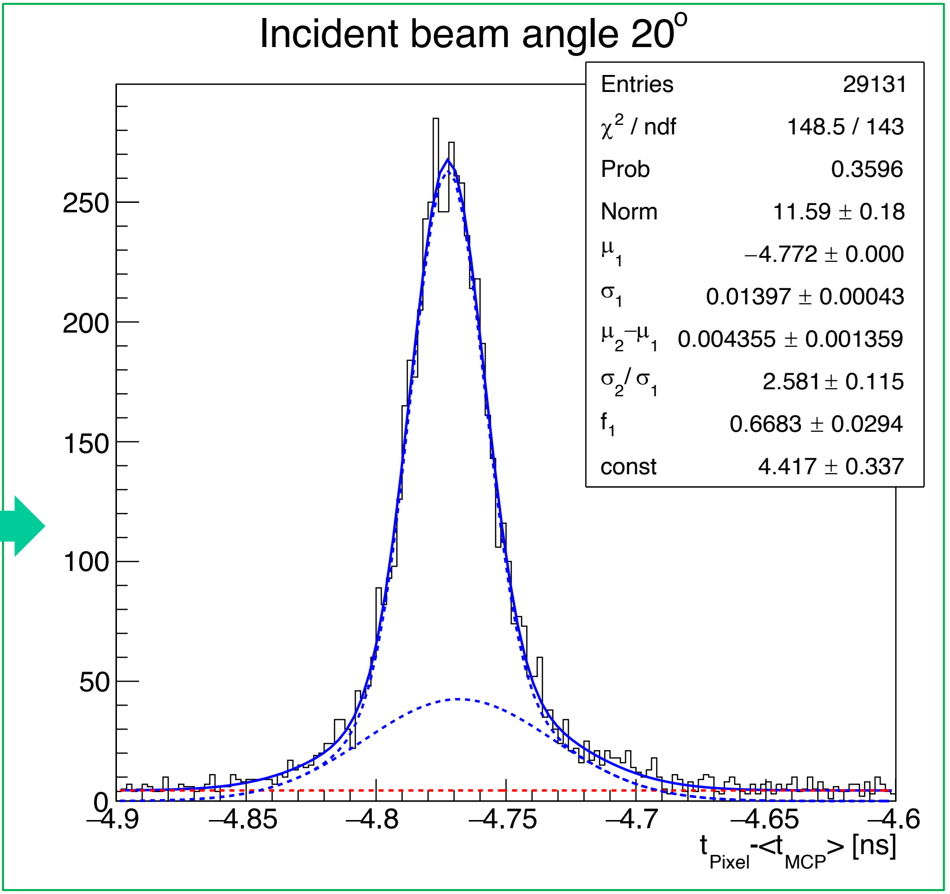

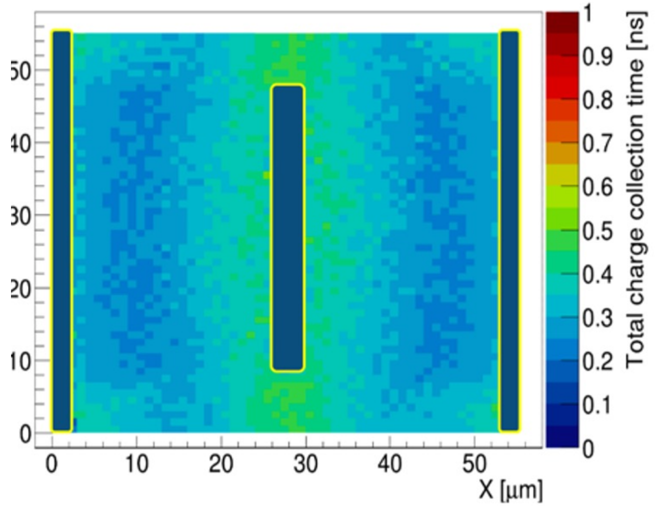

Simulated Time of arrival map of a single 3D-trench sensor pixel obtained in the lab by IR laser scan (α_{tilt} = 0°)

Tilting has the effect of «mixing up» the fast and less-fast regions of the pixels, thus uniforming the timing response

As a result, the shapes are more Gaussian at increasing α_{tilt}

Notice that, due to detection efficiency, α_{tilt} = 20° is the normal working condition of a 3D in a detecting system

Irradiated sensors – efficiency

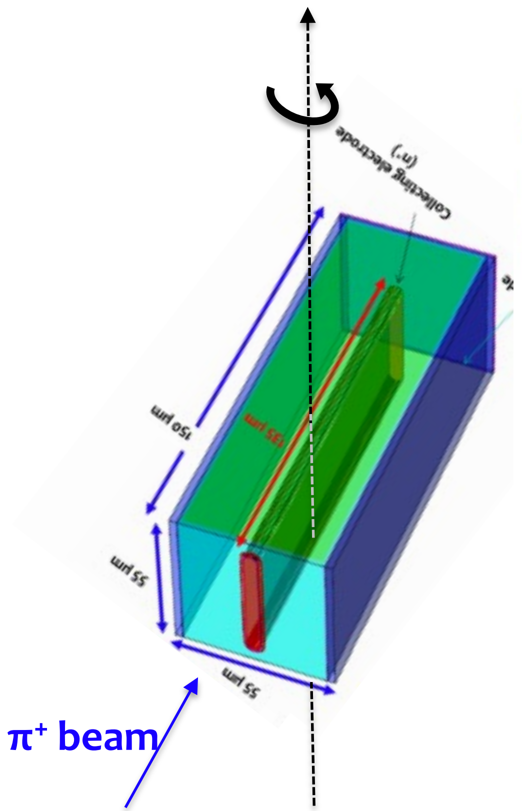

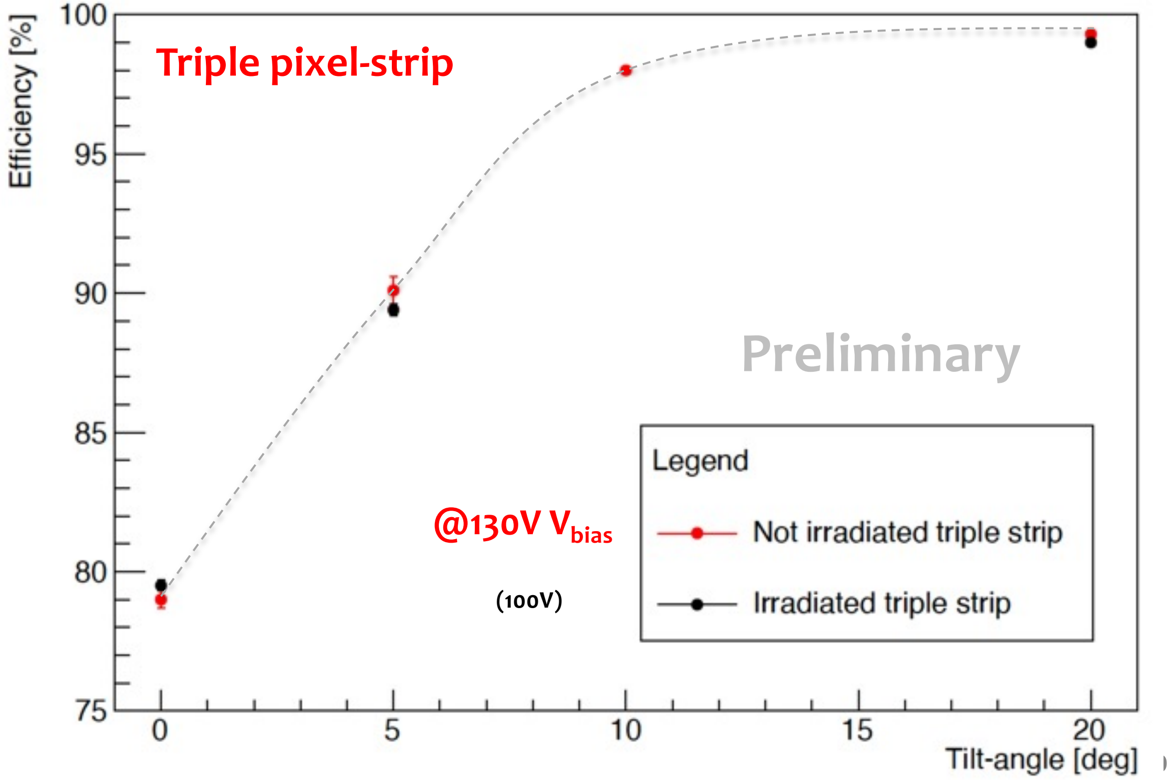

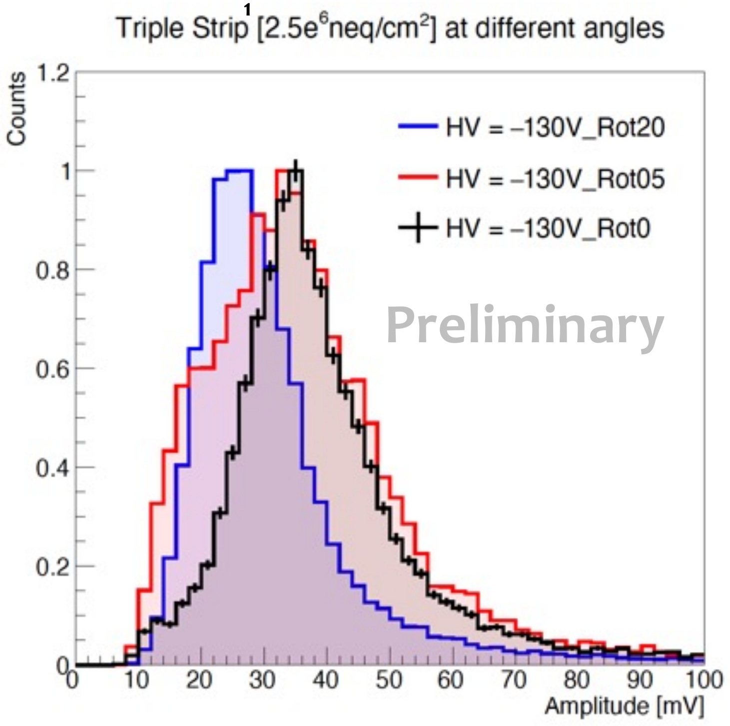

The inefficiency (at normal incidence) due to the dead-area of the trenches is fully recovered by tilting the sensors around the trench axis

also for sensors irradiated with fluences of $2.5 \cdot 10^{16}$ 1-MeV neutron equivalent

Time resolution of the irradiated pixel

@ SPS-H8 tests May '22

Not irradiated pixel at α_{tilt} = 0°

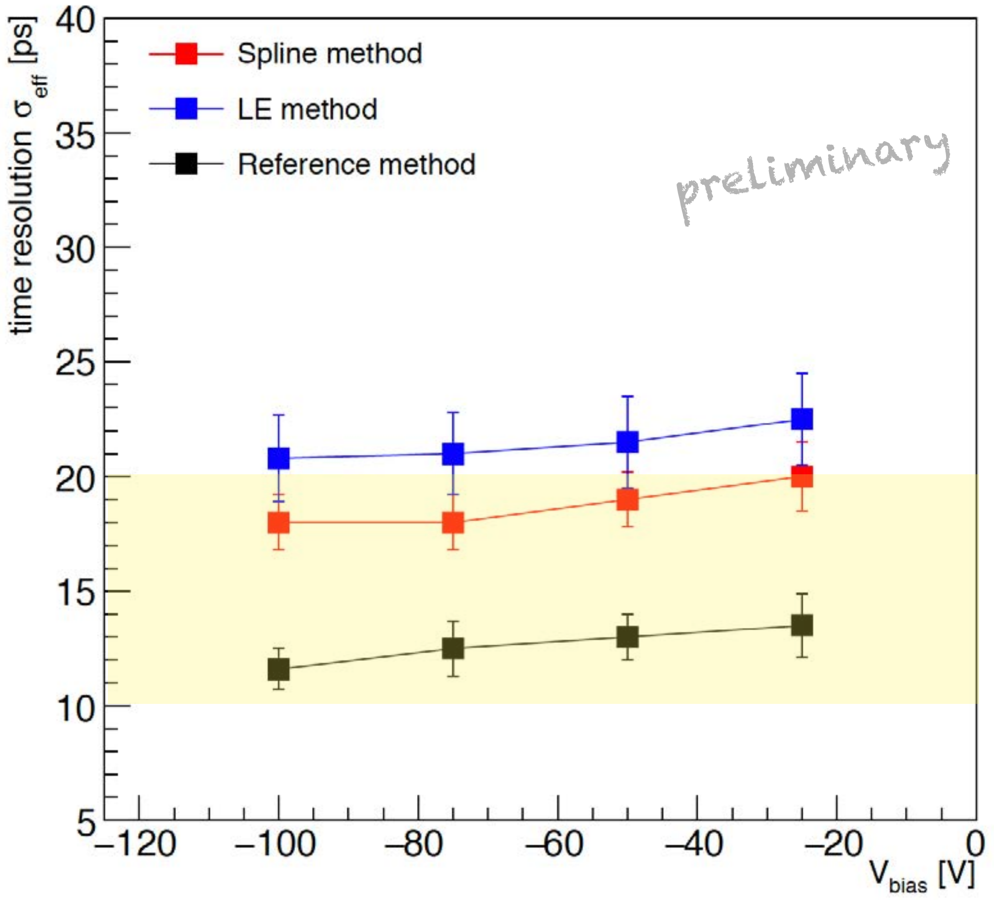

Irradiated pixel at 2.5 10^{16} 1 MeV n_{eq}/cm^2

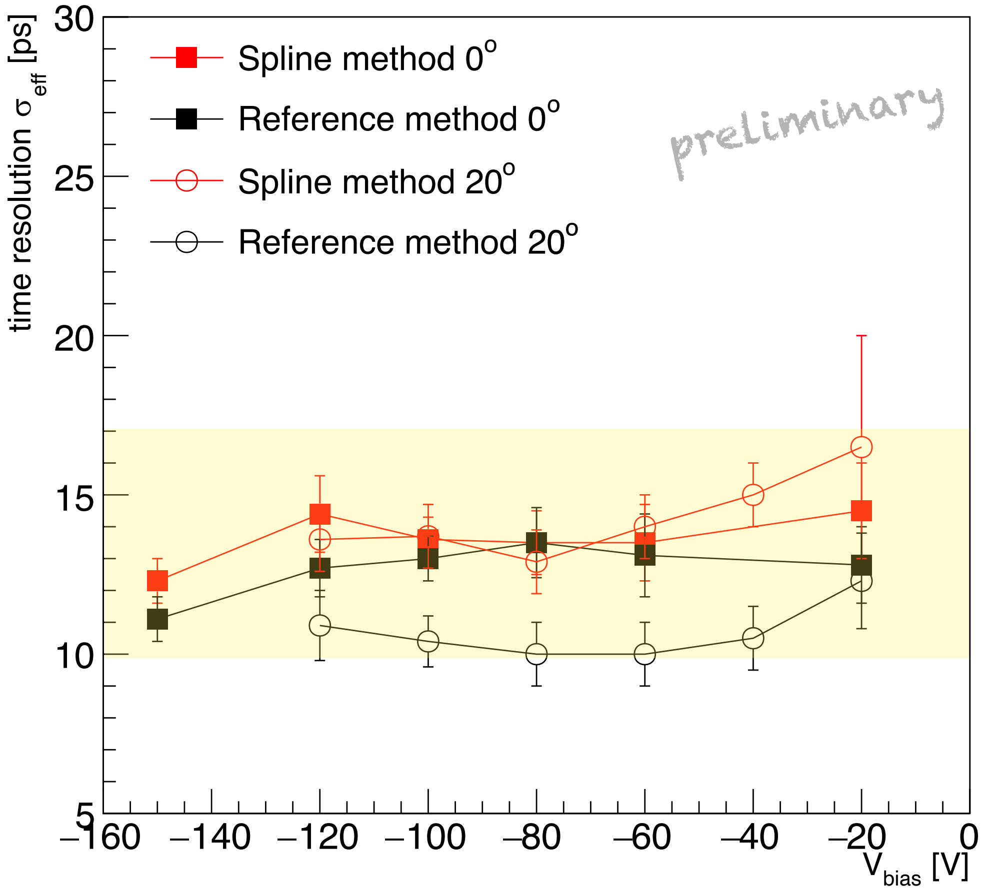

σ_{eff} ≈ 10-15 ps – still preliminary

With respect to the not-irradiated sample almost negligible differences, buta slight improvement appears (to be verified).
More analysis (and measurements) still necessary to understand the behaviour of the curves in detail

Irradiated sensors – timing performance

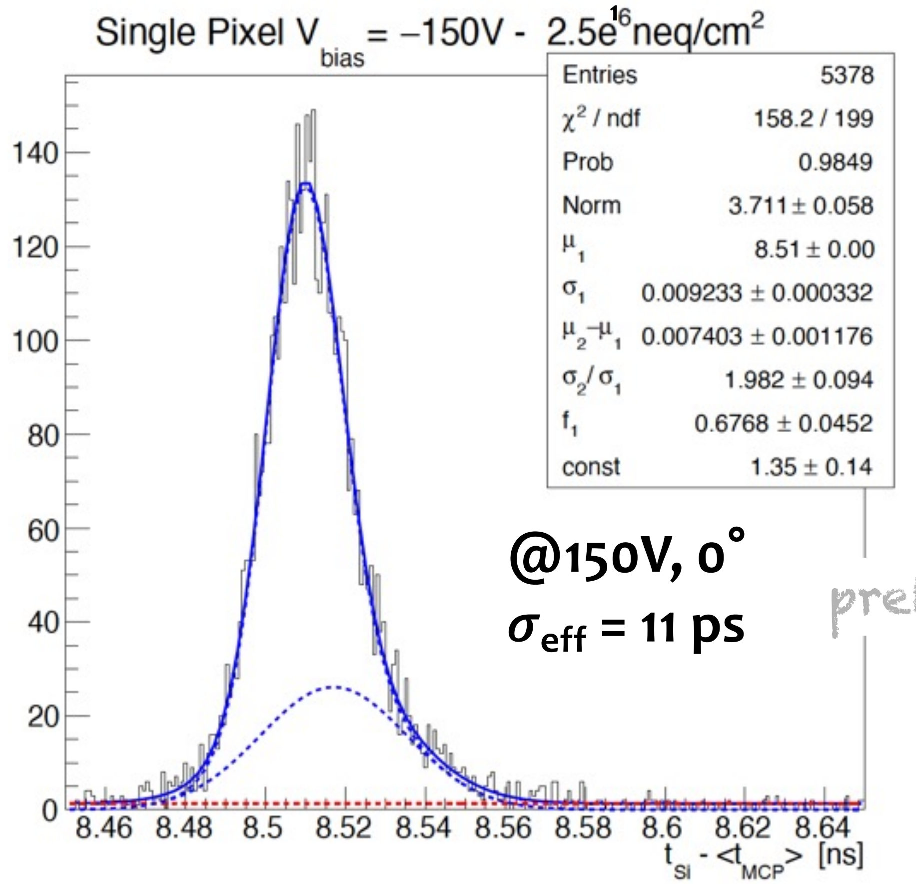

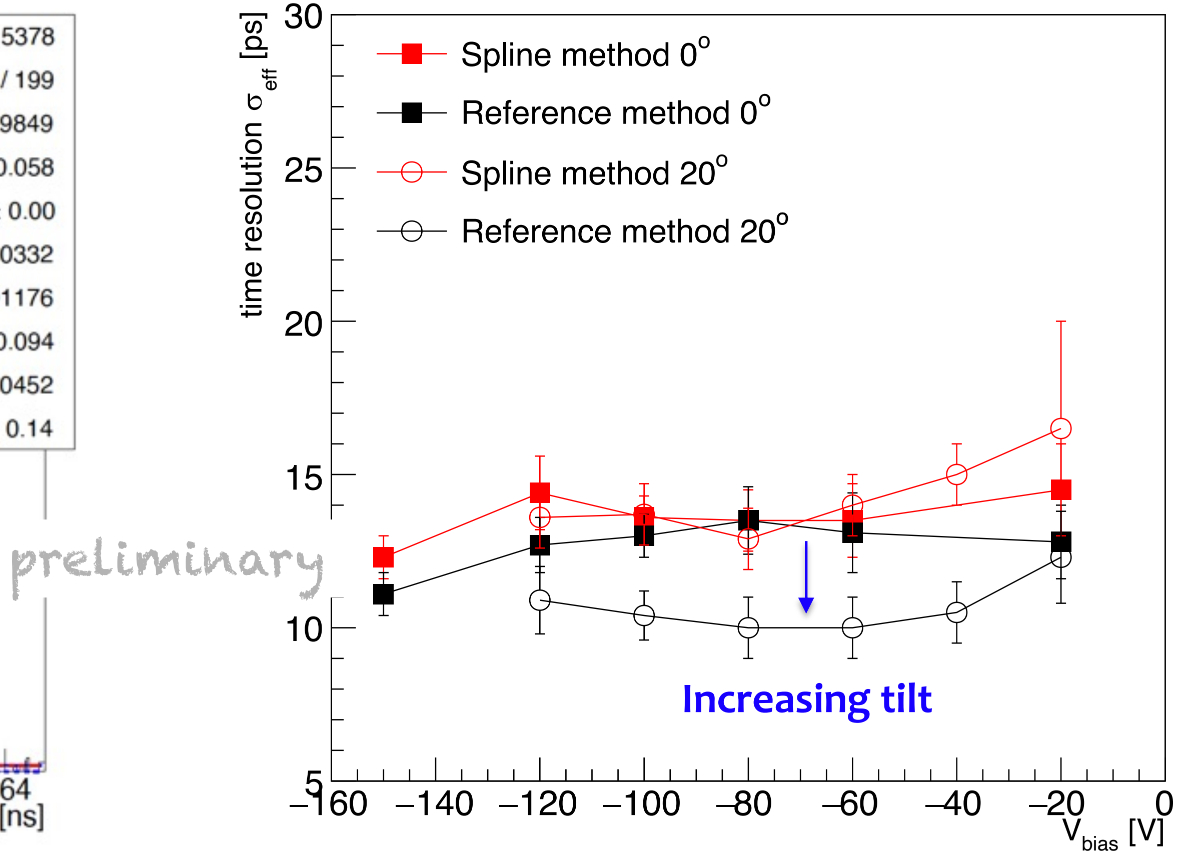

Excellent time resolution (σ_{eff} = 11 ps) measured at 150V on single pixels irradiated with fluences of **2.5·10^{16} 1-MeV n$_{eq}$/cm^2**

Again, there are indications that a tilted sensor even performs slightly better than at normal incidence

Summary

- 4D timing is a fundamental ingredient in the next-to-come experiements at colliders

- Several exciting development activities are on the way

- The specific structure of 3D sensors allows freedom of design and deep control of their operation, allowing maximum performance in timing

- Measurements on 3D sensors show excellent time resolution ($\sigma_t \approx$ 10 ps) and efficiency ($\varepsilon \approx 0.99$) both before and after heavy irradiation ($\geq 2.5\ 10^{16}\ n_{eq}/cm^2$). Their limit is still to be found

- Electronics is crucial for a timing system performance and is presently the limiting stage of the system. Developements are ongoing…

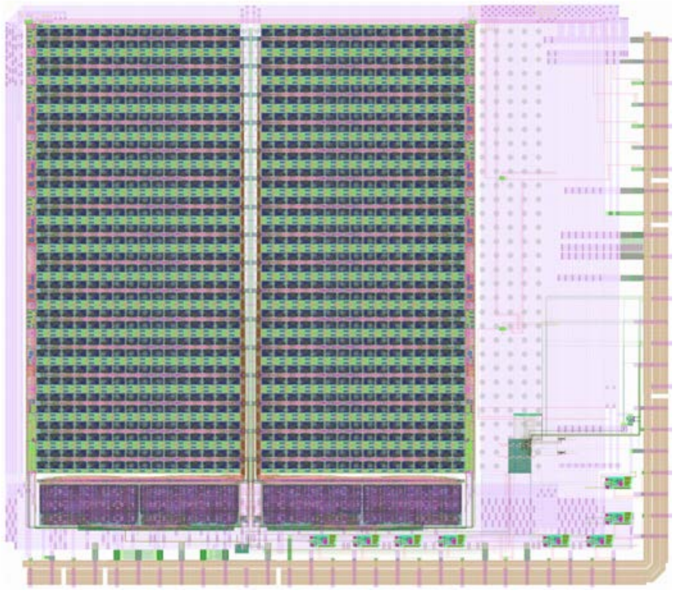

Timespot1 ASIC layout

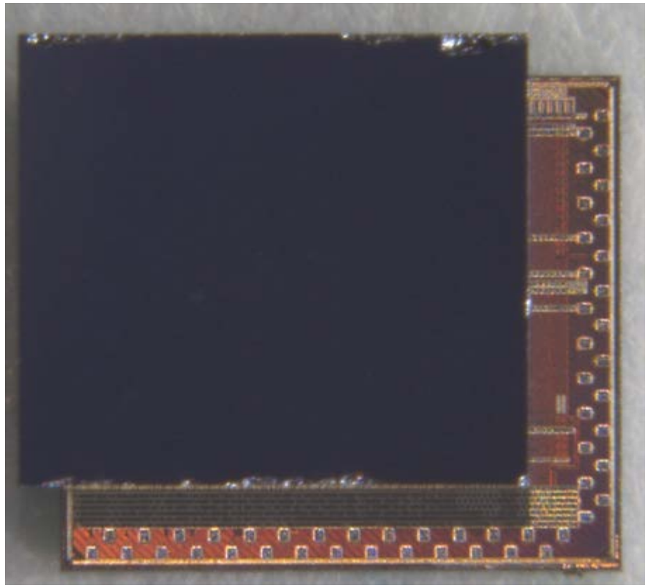

Timespot1 hybrid with 32x32 3D-trench matrix